Universitat Politecnica de Catalunya
Escola Tècnica Superior d'Enginyeria de Telecomunicació
Departament d'Enginyeria Electrònica

MASTER THESIS
of

Pietro Luigi Carotenuto

Supervised by Francisco Juan Guinjoan Gispert and Domingo Biel Sole

Grid impedance estimation in PV grid-connected systems through PQ variation methods. A Simulink-based approach

Escola Tècnica Superior
d'Enginyeria de Telecomunicació de Barcelona

Universitá degli Studi di Salerno

Barcelona, July 2011

To my wonderful mother
and my dear grandmother,
and to all those who
supported me
during my journey
coming up here…

"There is no favorable wind for the sailor who doesn't know where to go"

Seneca

Index

Introduction

In recent years the development and the steady increase of renewable sources, such as photovoltaic panels wind turbines or fuel cells, has required more advanced methods in order to improve the performances of grid-tied systems or the so called *distributed power generation systems*.

The term “Distributed Power Generation System” (DPGS) means that electric power is no more delivered to the utility only by the grid but also by special systems that convert the energy of local renewable sources into power that can be used by local loads or sent and sold to the electric grid operator. An example of micro-grid is shown in the figure 0.1.

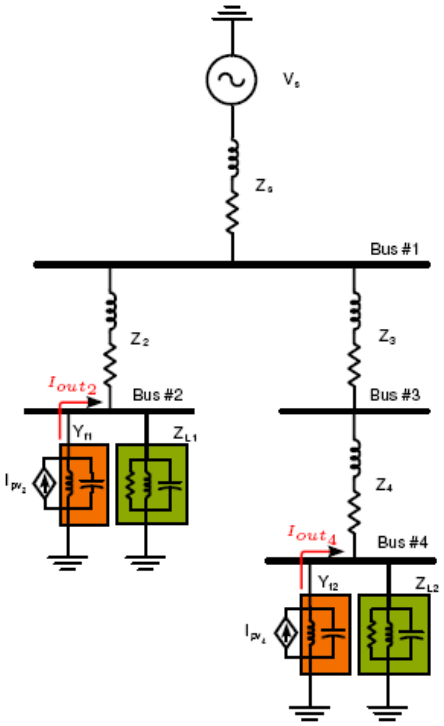

Fig. 0.1: A micro-grid model

The main issue is at the same time to acquire as much power as possible from local sources (for example tracking their output characteristic) and to manage this power in order to prevent undesired effects, such as the instability of the grid itself.

In fact, DPGS can have different topologies (the number of sources, their nominal power, the number of branch with their own line impedance…) and so every node in the grid can be disturbed in different ways by any change in the grid itself.

The main problem is that at the beginning DPGS were developed without using the same regulations in all countries; this means that, due to the more and more complex topologies of micro-grids, it was needed to develop new methods in order to ensure a minimal security (i.e. detecting as soon as possible faults and their location) and to estimate the margin of stability of the grid. As regards the human security, it is really necessary that, when an intentional or unintentional disconnection of the main grid happens, the local source is disconnected too in order to prevent the islanding condition: in this case a great voltage could appear to the local load and this is a very dangerous condition for technical staff who should detect some fault on the line (see the figure 0.2). So, different *anti-islanding* methods (see [5] [6]) have been developed in each country under different regulations, but, at the same time, in order to be applied to any micro-grid, it is very important the method complies with the most stringent standard requirements. An example of islanding prevention rule is given by the German standard VDE0126 for grid-connected PV systems requiring to isolate the supply within 5 seconds after an impedance change of 1 Ω (see [5]).

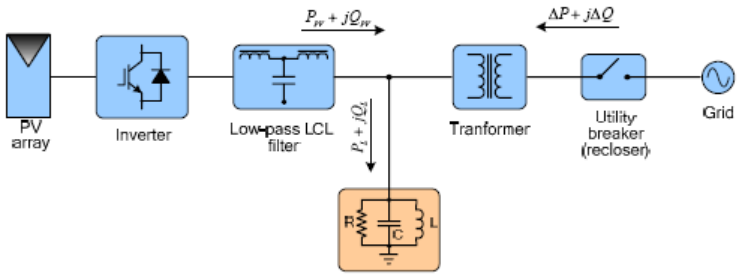

Fig. 0.2: The islanding operation phenomenon: once the grid is disconnected, all the power is reversed on the local load.

The stability margins of the grid are well estimated analyzing the grid model and developing new estimation methods of grid parameters (i.e. grid impedance).

0.1 Impedance estimation techniques

Any impedance estimation technique is made at least by two main steps: the measurement of currents and voltages and the post-processing of acquired data, typically involving a lot of mathematical calculations and the use of special hardware devices, since memorization and fast analysis of data are required.

Generally, the state of art classifies the methods for grid impedance estimation into two main categories: *passive* and *active* methods (see [7]).

Passive methods are based on monitoring line voltages and currents (i.e. signals that are already present in the system), their frequency… and on measuring of distortions can affect them; in this case, the main problem is that distortions could not be so large to be accurately measured, failing to give an exact estimation of the grid impedance: for this reason, it is known that passive methods have a very large *non-detection zone* (NDZ).

Active methods deliberately create a disturbance generally at the point of common coupling (PCC) and the grid impedance estimation is based on the grid response to the distortion. The most common disturbances could be summarized into three groups:

- *Current pulse transient* usually applied at zero crossing of the grid voltage. The grid impedance can be estimated measuring the voltage transient due to the injection of this signal. These methods are well suited to obtain fast results since the disturb is injected for a limited time only, but they involve high performance in A/D acquisition devices and must also use special numerical techniques to eliminate noise and random errors.
- *Non characteristic sub-harmonics (inter-harmonics)* injected into the grid before or at the PCC to estimate the grid impedance at a particular frequency (and at grid frequency) for example by considering the Discrete Fourier Transform of the injected current and of voltage response.
- *Power variations* of both active and reactive power that produce grid current and voltage variations basing on which the grid impedance can be estimated.

Active methods have generally a very small non-detection zone, but they suffer from a certain number of problems arising from actual implementation issues and limitations, mainly related to the rate of repeated injections that is normally kept high in order to increase the signal-to-noise ratio but, at the same time, that tends to increase the total harmonic distortions (THD); the accuracy is also reduced when the active methods are applied to the variable-frequency conditions of the grid.

Grid impedance estimation techniques can be also classified by considering the period of time during which the estimation is made by processing the acquired data. So, methods can be grouped into:

- *On-line* methods when impedance estimation is made just after measurement of current and voltage at the PCC and during the normal inverter operation. Generally they are the most interesting since the estimation is made in "real time" and parameters of inverters can be adjusted to improve the grid stability or in general the performance of micro-grid due to the changing operating conditions and various unforeseen factors associated with wide-area power systems.
- *Offline* methods when the estimation is made after all data have been acquired during a second phase and they are generally computer aided.

In this section different methods will be presented for the *on-line* grid impedance in photovoltaic grid-tied systems. So, a method will be chosen, well explained and implemented using MATLAB®/Simulink software.

Passive methods are generally not so useful in photovoltaic systems due to the fact that not so much disturbs appear respect to others renewable (mechanical) sources, i.e. the wind turbines.

Online algorithms should be causal for real-time implementation and, in order to improve their spatial and temporal complexity, should be recursive.

Yang *et al.* proposed in [1] a method to estimate the impedance matrix measuring in synchronous voltages and currents in a multi-source multi-load grid model using *phasor measurement units (PMUs)* and using these data in a recursive least square algorithm with *forgetting factors*.

Since the synchronization of measurements is fundamental for the correctness of estimation, in a practical implementation of the method it can be guaranteed by using GPS synchronous clock signals. The authors were able to simplify the calculus of the least square algorithm in order to reduce the spatial and time complexity, since the grid could be very large and the calculations could take a very long time. But, at the same time, a very large number of measurements and their high rate of changes are required in order to improve the correctness of estimation. Yang *et al.* introduced forgetting factors to reduce the influence of past measured data on the current estimated matrix in order to be more efficient to detect grid changes without reduce the precision of the measure.

The method proposed by Yang *et al.* is based on synchronized phasor measurements and it needs special hardware devices at every node in the grid whose topology should be known in advance. The advantage of this algorithm is that no injection of signal or variations of any kind

are applied: the parameters of grid are estimated only by monitoring bus voltages, load voltages and currents and by using their variability.

Generally, the active methods lack of synchronization between the different network nodes: in particular a situation of instability (and high inaccuracy) can be verified if many grid connected inverters are injecting disturbing signals at the same time. The instability of the grid could happen if, since a bad estimation of grid impedance is made, the inverter's parameters are incorrectly adjusted.

Liserre *et al.* proposed in [2] a method to detect the grid impedance exciting the resonance of LCL-filter. The idea is to exploit the frequency characteristic of the current controlled inverter (i.e. the frequency response of i/i* currents ratio, where i* is a reference current) in order to have an indication of grid impedance value. Generally the current response can be sensed at the grid side or at converter side (if the LCL-filter is not integrated into the controller).

There is some limitation due to the fact the LCL-filter introduces instability if not properly damped. This method is not based on the injection of as signal but on the use of the natural resonance of the LCL-based system that is particularly sensitive to the grid impedance changes.

Due to the nature of this approach, the values of the inductor and of capacitor affect the performance since the frequency response is obviously related to the position of zeros and poles.

The LCL-filter can be excited in three different ways:

- Increasing the proportional gain of the current control
- Add other zeros and poles in the controller in order to push out the LCL-filter poles out of the stability region
- Saturate the ac voltage command for the PWM modulator

The basic idea is always introduce instability in the system. The detection of the peak resonance could be made by using FFT or resonant controllers.

This method has the advantage of reducing the total harmonic distortion since measurements are made only periodically but at the same time it has the disadvantage that the calculation of DFT itself can overload the DSP where it has been implemented.

Generally estimation by active methods is made by injecting a proper voltage disturbance to the reference voltage of the PWM modulator and measuring the current response.

Shen *et al.* proposed in their paper [3] to implement a new different approach to the standard technique: since generally the current response to the inter-harmonic disturbance is quite small compared with the grid voltage and a delicate sensor should be used due to the presence of background distortions and noise, it has been proposed to measure the inter-harmonic disturbance within the digital processor. The inter-harmonic current response can be extracted with Discrete Fourier Transform (DFT) analysis. The inter-frequency signal is at 75Hz with a grid frequency of 50Hz.

A possible limitation is that this method involves the knowledge of an initial grid impedance. This method can be also extended using the grid voltage feed-forward and in this case the grid impedance is obtained by changing of the feed-forward coefficient.

Shen *et al.* proposed also a current control optimization using weighted coefficients for the sensed filter current: if these values are correctly detected through repetitive grid impedance estimations, the control system with LCL-filter can be degraded from 3^{rd} order to 1^{st} order suppressing the resonant peak without a significant passive damping of the filter. By this way, the stability of the system is ensured.

This technique can be implemented with the existing sensors and the existing digital processor of the inverter and it provides a low cost and adaptive approach for current control of grid-tied inverters, especially for weak grids which always have a wide range of line impedance.

It has been observed that current injection is more advantageous respect to voltage injection: if a current disturbance is injected, the current controller must track the inter-harmonic signal too and the current control loop response depends only by parameters and by structure of the controller itself; the output filter and the grid inductance values don't affect the current rise time on the contrary of voltage injection where the generated current is seen as a disturbance and the system tents to reject that component. So, in the case of current injection, the response time is more predictable and the tuning of the estimation algorithm is easier.

Generally, the grid impedance estimated by a signal injection is calculated at the inter-harmonic frequency as the ratio between the DFT of grid voltage and the DFT of the grid current. As stressed before, the algorithm used to implement the DFT affects the performances of the method. Many DFT algorithms have been proposed in literature.

Instead of using a standard running sum approach to calculate the DFT, Petrella *et al.* in [4] implemented an impedance estimation technique that is based on a moving window DFT that has the advantage of reducing the time required for the estimation respect to the standard

method. A good accuracy of the estimation is well guaranteed by repeating estimations and by averaging results in order to reduce the effects of harmonic distortions of the grid.

The used frequency resolution ($\Delta f = 25Hz$) allows the accurate detection of any voltage/current harmonic component being an integer multiple of grid or injected frequency. All other components appear as spectral leakage.

The spectral leakage is produced also when a non-integer ratio between grid frequency and DFT sampling frequency is chosen. They proposed to reduce spectral leakage by a virtual real time adaptation of the sampling period of the DFT: at first the signal is sampled at high frequency, and then filtered by using a digital anti-aliasing filter with a cut frequency equal to half of the sampling frequency of DFT; then obtained samples are down-sampled and non-synchronous samples are numerically interpolated.

The estimation of grid impedance is given by ratio of the DFT of voltage response at inter-harmonic frequency and the DFT of injected current at the same frequency. In order to get the estimation at the grid frequency, the reactance of the previous estimation should be multiplied by grid frequency and divided by inter-harmonic frequency. The validity of the measure is guaranteed by having the grid frequency very near to the inter-harmonic frequency.

Active and reactive power variation can be used in order to estimate the grid impedance of a single phase system, as Ciobotaru *et al.* proposed in their paper [5]. By using a synchronous reference system for grid voltage and current, the grid resistance and grid inductance can be easily calculated by changing active and reactive power variation.

The basic idea is to change the working point and to be able to estimate the grid impedance by measuring the variations of synchronous voltages and currents from the previous values taken as reference.

The assumption of this method is that the grid impedance is *linear* and that both the grid impedance and the grid side voltage don't change during the measurements.

The PQ variation method has been tested under different conditions of total harmonic distortion and under grid impedance step variation in order to verify the compliance to the anti-islanding standard requirements.

The PQ variation method proposed by Ciobotaru *et al.* in their paper [5] has been deeply analyzed and all contents presented in this Thesis are based on this work: sometimes, referring to the method proposed by Ciobotaru, it will be referred to it as the *original* method.

As mentioned at the beginning, all these estimation methods should comply with the standard requirements for islanding detection and human safety. These so-called *interconnection standards* are the effect of a great change in power generation trends from last years of 20th century until today, since more and more the idea of having a unique big power manufacturer and distributor has been reversed into the real possibility to install and use own small local plant. So, the aim of these interconnected standards is also to encourage electricity customers to become electricity producers too.

These standards, such as the American IEEE 1547 or the German VDE0126, concern:

- Voltage requirements: if the utility voltage is outside certain limits (typically around ± 15 %) the inverter should stop to energize within 0.16 to 2 seconds (depending on the standards). More sever under/over voltages lead to shorter intervention times.
- Frequency requirements: if the utility frequency is outside certain limits (typically around ± 1 %) the inverter should stop to energize the utility line within 0.16 seconds.
- dc current injection (especially for tranformerless structures)
- earth current
- anti-islanding
- the total harmonic distortion

The differences between the requirements concern the range of voltage or frequency values and the clearing time.

In effect, these requirements guarantee that the power factor is above a minimum value that is generally 85% or, in some case, they require strongly a unitary power factor (it means zero reactive power).

0.2 Objectives of the work

All the presented techniques have been analyzed and, despite they are all interesting to study, the PQ variation method has been chosen to be implemented using Matlab®/Simulink.

The choice of the PQ variation method is due to the following considerations:

- No injection of a signal is needed: the total harmonic distortion is not increased by burst injection; only active and reactive power fluctuations are present.
- No Discrete Fourier Transform algorithm is needed since it is not necessary to analyze any frequency spectrum: it means that the DSP memory or processor is not overloaded.
- The PQ variation method is simply based on the control of the reference current in order to change active or reactive power.
- No phase analysis of signals is needed: even if the estimation involves the phasors, the synchronous reference frame transforms the sinusoidal variables into DC values, more easy to be analyzed. So the formulas used to estimate the grid impedance depend only by grid current and voltage scalar variation values.
- The method, since it consists of few steps, can be easily implemented on a cheapest hardware device.

The Master Thesis has been organized into the following chapters:

- Chapter 1: the PQ variation method is presented and its validity is discussed
- Chapter 2: the implementation of the presented method by switched and averaged model in Matlab®/Simulink
- Chapter 3: the results of simulations
- Chapter 4: a new modified version of PQ variation method is implemented in order to overcome the standard method limitations and its application to a micro-grid is analyzed
- Conclusions

Chapter 1

The PQ variation method

1.1. An historical overview

The purpose of these first two paragraphs is introducing the original Akagy's theory, initially applied only to three-phase systems, and to analyze the subsequent developments of this theory and its generalization to multi-phase circuits. Then, the applicability to the single-phase systems is deduced as a special case of poly-phase system.

In 1983 Akagi *et al.* proposed a new theory about the control of active filters in three-phase power systems called "Generalized Theory of the Instantaneous Reactive Power in Three-Phase Circuits" or also known as the "p-q Theory", as illustrated in [8][9].

Since the proposed method of this work uses the "p-q Theory" applied to single phase systems, it is necessary to introduce some concepts about it.

In fact, the Akagy's theory has been developed more and more and extended by other researchers to be applied into many scenarios, for example in the case of three-phase power systems without energy storage (giving a way to easily analyze the compensation of reactive power) and into poly-phases circuits.

The figure 1.1 represents a three-phase system with neutral wire: the Z_1, Z_2 and Z_3 are the load

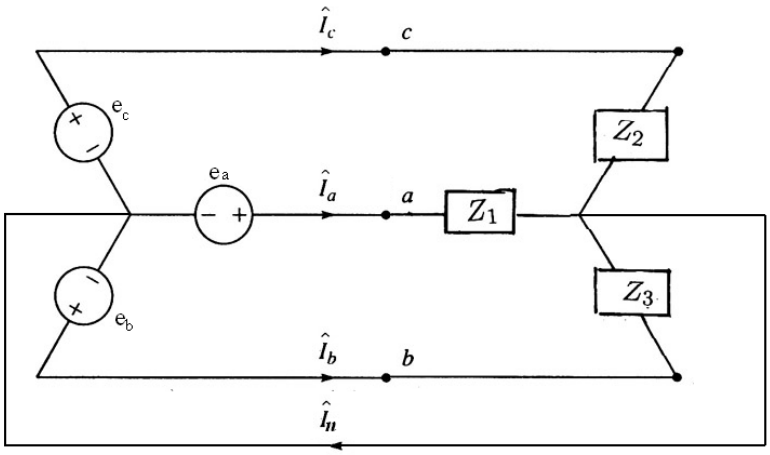

Fig. 1.1: A four-wire three-phase system

impedances while the line impedances are neglected so that e_a e_b and e_c are also the load voltages; the I_a I_b and I_c are the three-phase currents, whose expressions are:

$$\begin{cases} I_a = I\sqrt{3}\,\sin(\omega t + \varphi) \\ I_b = I\sqrt{3}\,\sin\left(\omega t + \varphi + \frac{2}{3}\pi\right) \\ I_c = I\sqrt{3}\,\sin\left(\omega t + \varphi - \frac{2}{3}\pi\right) \end{cases} \tag{1.1}$$

while I_n is the neutral current that is given by:

$$I_n = I_a + I_b + I_c \tag{1.2}$$

Obviously, if the three-phase system has a balanced load (i.e. Z_1=Z_2=Z_3), the neutral current will be equal to zero.

Also the voltage generators have the same expressions:

$$\begin{cases} e_a = E\sqrt{3}\,\sin(\omega t + \theta) \\ e_b = E\sqrt{3}\,\sin\left(\omega t + \theta + \frac{2}{3}\pi\right) \\ e_c = E\sqrt{3}\,\sin\left(\omega t + \theta - \frac{2}{3}\pi\right) \end{cases} \tag{1.3}$$

From the neutral current, the so-called homopolar current is calculated as:

$$I_0 = {}^{1}/_{\sqrt{3}}(I_a + I_b + I_c) = \frac{I_n}{\sqrt{3}} \tag{1.4}$$

which is a measure of imbalance of the system.

In order to separate the instantaneous homo-polar component from the other power components (see eq. 1.7 – 1.10), Akagy used a stationary reference frame (the so-called *0αβ* or *Clarke Transformation,* see eq. 1.5). By this way, the *three-phase abc* voltages and currents of the three-phase system are transformed into a two-phase orthogonal (stationary) system. Then, two orthogonal components of the electrical power are calculated using the 0αβ variables too: the so-called active power P and the reactive power Q.

So, the voltages and the currents can be transformed by an appropriate Clarke's matrix C:

$$C = \sqrt{\frac{2}{3}}\begin{bmatrix} \frac{1}{\sqrt{2}} & \frac{1}{\sqrt{2}} & \frac{1}{\sqrt{2}} \\ 1 & -\frac{1}{2} & -\frac{1}{2} \\ 0 & \frac{\sqrt{3}}{2} & -\frac{\sqrt{3}}{2} \end{bmatrix} \quad , \quad \begin{bmatrix} e_0 \\ e_\alpha \\ e_\beta \end{bmatrix} = C \begin{bmatrix} e_a \\ e_b \\ e_c \end{bmatrix} \quad , \quad \begin{bmatrix} i_0 \\ i_\alpha \\ i_\beta \end{bmatrix} = C \begin{bmatrix} i_a \\ i_b \\ i_c \end{bmatrix} \tag{1.5}$$

In a three-phase system with neutral wire, the instantaneous real power is given by:

$$p(t) = e_\alpha i_\alpha + e_b i_b + e_c i_c = e_0 i_0 + e_\alpha i_\alpha + e_\beta i_\beta \quad (1.6)$$

Akagy introduced two instantaneous real powers p_0 and $p_{\alpha\beta}$ and an instantaneous imaginary (or *reactive*) power $q_{\alpha\beta}$. The differences between the real and imaginary powers are due to the phases involved into their calculus. These instantaneous values are expressed by the following matrix relationship:

$$\begin{bmatrix} p_0 \\ p_{\alpha\beta} \\ q_{\alpha\beta} \end{bmatrix} = \begin{bmatrix} e_0 & 0 & 0 \\ 0 & e_\alpha & e_\beta \\ 0 & -e_\beta & e_\alpha \end{bmatrix} \begin{bmatrix} i_0 \\ i_\alpha \\ i_\beta \end{bmatrix} \quad (1.7)$$

So:

$$p_0 = e_0 i_0 \quad (1.8)$$

$$p_{\alpha\beta} = e_\alpha i_\alpha + e_\beta i_\beta \quad (1.9)$$

$$q_{\alpha\beta} = -e_\beta i_\alpha + e_\alpha i_\beta \quad (1.10)$$

The instantaneous powers p_0 and $p_{\alpha\beta}$ are called *real* because their components belong to the same phase and, for this reason, their dimension is Watt [W]. Instead, the $q_{\alpha\beta}$ power components are calculated as the product of instantaneous voltage in one phase and the instantaneous current in another phase, so its dimension is Volt-Ampere-reactive [Var].

The matrix (eq. 1.7) is often referred also as a “mapping matrix” since it gives the relationship between a three-dimensional current space and a three-dimensional power space.

By inverting this matrix, the stationary currents can be expressed by active and reactive powers and 0αβ voltages, as shown:

$$\begin{bmatrix} i_0 \\ i_\alpha \\ i_\beta \end{bmatrix} = \frac{1}{e_0 e_{\alpha\beta}^2} \begin{bmatrix} e_{\alpha\beta}^2 & 0 & 0 \\ 0 & e_0 e_\alpha & -e_0 e_\beta \\ 0 & e_0 e_\beta & e_0 e_\alpha \end{bmatrix} \begin{bmatrix} p_0 \\ p_{\alpha\beta} \\ q_{\alpha\beta} \end{bmatrix} \quad (1.11)$$

where $e_{\alpha\beta}^2 = e_\alpha^2 + e_\beta^2$. (1.12)

So, solving the matrix, the instantaneous currents are obtained:

$$i_0 = \frac{p_0}{e_0} \tag{1.13}$$

$$i_\alpha = \frac{e_\alpha p_{\alpha\beta} - e_\beta q_{\alpha\beta}}{e_{\alpha\beta}^2} = i_{\alpha p} + i_{\alpha q} \tag{1.14}$$

$$i_\beta - \frac{e_\alpha q_{\alpha\beta} + e_\beta p_{\alpha\beta}}{e_{\alpha\beta}^2} - i_{\beta p} + i_{\beta q} \tag{1.15}$$

where

- i_0 is the zero-sequence (or homo-polar) instantaneous current
- $i_{\alpha p}$ and $i_{\beta p}$ depend on the active power
- $i_{\alpha q}$ and $i_{\beta q}$ depend on the reactive power

It is really important to notice that the "mapping matrix" can be inverted only if $e_0 \neq 0$ but, in any case, since the i_α and i_β currents are independent from the e_0 value, this method can be also extended to the three-phase systems without neutral wire as well as to single-phase systems (and in general to a poly-phase system).

It is simple to demonstrate that instantaneous active power is given by multiplying voltages and currents having the same 0-α-β phase while the instantaneous reactive power is zero:

$$e_0 i_0 + e_\alpha i_{\alpha p} + e_\beta i_{\beta p} = e_0 i_0 + e_\alpha \left(\frac{1}{e_{\alpha\beta}^2} e_\alpha p_{\alpha\beta} \right) + e_\beta \left(\frac{1}{e_{\alpha\beta}^2} e_\beta p_{\alpha\beta} \right) =$$

$$= p_0 + p_{\alpha\beta} = p_0 + p_{\alpha p} + p_{\beta p} = p \tag{1.16}$$

$$e_\alpha i_{\alpha q} + e_\beta i_{\beta q} = e_\alpha \left(-\frac{1}{e_{\alpha\beta}^2} e_\beta q_{\alpha\beta} \right) + e_\beta \left(\frac{1}{e_{\alpha\beta}^2} e_\alpha q_{\alpha\beta} \right) = p_{\alpha q} + p_{\beta q} = 0 \tag{1.17}$$

The figure 1.2 shows more clearly the power components of active and reactive power.

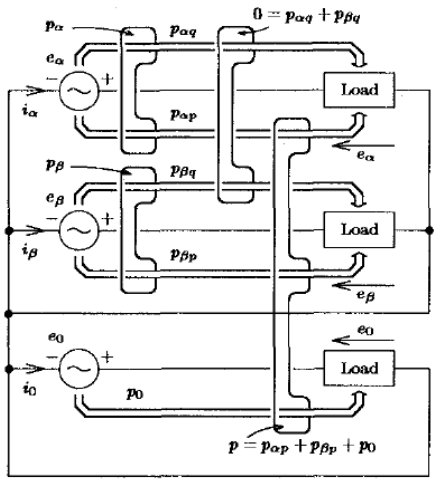

Fig. 1.2: graphical representation of involved power components

Referring to three-phase systems *without energy storage*, this is an expected result, since the active power p cannot change and the only way to reduce the losses is guarantee that imaginary power q is zero.

1.2. The p-q Theory applied to poly-phase systems

Once the original p-q Theory has been introduced, its extension to poly-phase system can be considered and the applicability of the method to single-phase systems can be demonstrated as a special case of multi-phase systems.

The original work of Akagy can be extended (as illustrated in [10]) to be applied to a system with any number of phases. If m is an arbitrary number of phases and if the instantaneous voltages and currents of the m lines are represented by an m-dimensional vector *i(t)* and *v(t)*, the instantaneous power *p(t)* is the scalar product of these vectors:

$$p(t) = v(t)^T i(t) \tag{1.18}$$

where T is the symbol of matrix transposition.

The generic phase current i(t) can be expressed as the vector given by two components $i_p(t)$ and $i_q(t)$ where $i_p(t)$ is the orthogonal projection of i(t) on the vector v(t) and $i_q(t)$ is given by the difference between i(t) and $i_p(t)$ and it is obviously orthogonal to the vector v(t).

This means that:

$$p(t) = v(t)^T i(t) = v(t)^T \left(i_p(t) + i_q(t)\right) = v(t)^T i_p(t) \tag{1.19}$$

since $v(t)^T i_q(t) = 0$ due to the orthogonality of these vectors.

So, by deducing the dependence from power:

$$p(t) = v(t)^T i(t) = v(t)^T i_p(t) \tag{1.20}$$

$$i_p(t) = \frac{v(t)^T i(t)}{|v(t)|^2} v(t) = \frac{p(t)}{|v(t)|^2} v(t) \tag{1.21}$$

and remembering that $i_q(t) = i(t) - i_p(t)$ (1.22)

$i_p(t)$ and $i_q(t)$ can also be defined as the instantaneous active and reactive currents respectively.

Summarizing, the active and reactive power can be expressed by:

$$p(t) = v(t)^T i_p(t) \tag{1.23}$$

$$|q(t)| = |v(t)| \cdot |i_q(t)| \tag{1.24}$$

where the meaning of q(t) lies in a transfer of power between all phases without involving any power transfer to the load: again, it's clear that, considering no energy storage, the only way to reduce the losses is equating q(t) to zero.

The reactive power q(t) can be also seen as the vector product of voltage and current vectors: so it's orthogonal to the plane defined by voltages and currents. The sign associated to the reactive power q(t) is the direction of this vector respect to that plane. In some case (i.e. the single-phase system) the sign associated to q(t) is not so important.

The same results obtained by Akagy can be obtained by developing the previous equations in a simplest case, i.e. a two-phase system (m=2):

$$i_p(t) = \frac{p(t)}{|v(t)|^2} v(t) = \frac{v_\alpha(t)}{v_\alpha(t)^2 + v_\beta(t)^2} p(t) + \frac{v_\beta(t)}{v_\alpha(t)^2 + v_\beta(t)^2} p(t) = i_{\alpha p}(t) + i_{\beta p}(t) \tag{1.25}$$

$$i_q(t) = \frac{q(t) \times v(t)}{|v(t)|^2} = \frac{-v_\beta(t)}{v_\alpha(t)^2 + v_\beta(t)^2} q(t) + \frac{v_\alpha(t)}{v_\alpha(t)^2 + v_\beta(t)^2} q(t) = i_{\alpha q}(t) + i_{\beta q}(t) \tag{1.26}$$

The single-phase case is contained in the previous analysis: in fact, the instantaneous grid current i(t) is always equal to $i_p(t)$ while the instantaneous reactive current shouldn't exist.

1.3. A basic approach to the PQ variation method

Once the original "p-q Theory" and some further development have been analyzed and their validity has been demonstrated not only for the three-phase systems but also for an arbitrary poly-phase (and so single-phase) system, the proposed estimation method based on Akagy's work can be illustrated.

Analyzing the Akagy's Theory, it has been shown that the effects of active and reactive power on the line currents can be decoupled by considering the orthogonal projections of the current vector on the voltage vector in a generic poly-phase system.

The PQ variation method is based on the previous hypothesis applied to a single-phase system.

From an abstract point of view, a single-phase grid connected system is basically represented by a grid voltage generator V_g and by the Thevenin model of grid network itself: the former is the voltage measured at the "Point of Common Coupling" (for this reason sometimes Vg is called V_{PCC}) between the inverter's filter and the utility; the latter is composed by a grid impedance Z_g (whose resistive and inductive values are predominant) and by a grid-side sinusoidal voltage generator V_s.

The following figure shows the abstract circuit model where the voltage and the current perfectly in phase and a noise-free scenario are considered:

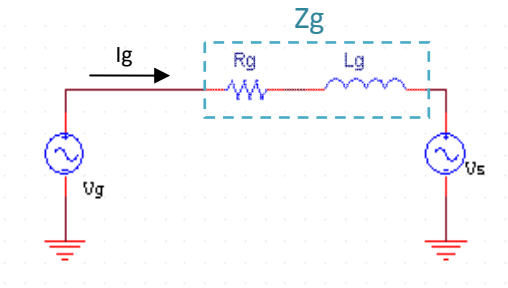

Fig. 1.3: an abstract representation of a single-phase system

The inverter of the local source is normally piloted so that V_g and I_g have zero phase-shift: in ideal conditions, all power generated is absorbed by the grid and the average reactive power is zero. Indeed, the instantaneous reactive power is never zero, since harmonic distortions appear, due to the regular switching operations of inverter.

The basic idea is to generate an appropriate reference current for the grid current in order to change properly the active and reactive grid power and to estimate the line impedance by measuring the voltage and current (scalar) variations respect to the reference values at the Point of Common Coupling (PCC).

The reference current depends on active and reactive reference power and on grid voltage stationary values.

The PQ variation method uses both *Clark* and *Park transformation*: the former is needed in order to generate two sinusoidal grid voltage components ideally having the same amplitude

but 90º degrees shifted; the latter is used in order to make an orthogonal projection of both grid voltage and grid current on a rotating axis that has the same angle and angular velocity of the grid voltage. By this way, for every variable, two components are obtained: a *direct* component that, if no disturb appear, represents the amplitude (DC value) of the involved variable and a *quadrature* component that must be equal to zero if the inverter works ideally and that could represent a measure of the disturbs in the grid. It will be demonstrated that the direct and the quadrature components depend only on active and reactive power respectively (see eq. 1.).

As previously mentioned, the reactive power is the amount of input power that is not transferred to the load: this concept is valid in single-phase systems too. The sum of active and reactive powers must be always equal to input power (i.e. a constant).

The active and reactive reference power values differently affect the reference current: the former acts on its amplitude by maintaining the reference current in phase with grid voltage if zero reactive power is required; the latter acts only on the phase of reference current.

Indeed, in order to demonstrate these concepts, some important principle of Power Theory should be re-called.

The complex power S is defined as:

$$S = VI^* = V\angle\theta_V \cdot I\angle\theta_I = VI\angle(\theta_V - \theta_I) \tag{1.27}$$

where V and I are rms values. Using a vectorial representation, it can be decomposed in an active and reactive power factors (the so-called P and Q):

$$S = VI\angle(\theta_V - \theta_I) = VI\cos(\theta_V - \theta_I) + jVI\sin(\theta_V - \theta_I) = P + jQ \tag{1.28}$$

where:

$$\begin{cases} P = Re(S) = VI\cos(\theta_V - \theta_I) = VI\cos\theta \\ Q = Im(S) = VI\sin(\theta_V - \theta_I) = VI\sin\theta \end{cases} \tag{1.29}$$

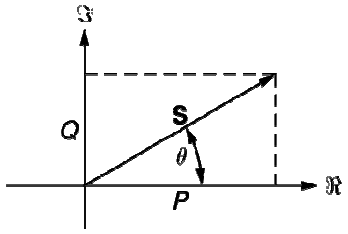

Fig. 1.4: The vector representation of the complex power S

Simply starting from this equation, it is now clear that, in order to change the active and reactive power measured at the Point of Common Coupling, it is possible to act both on amplitude and phase (shift) of voltage and current vectors.

Indeed, in order to give the maximum power transfer to the load, the grid voltage and the grid current must be always in phase (so the phase shift θ is equal to 0) and only the amplitude of the current should be adjusted in order to get the expected active power; instead, by increasing properly both the phase shift value and the amplitude of complex power S, the desired reactive power is acquired without having active power variation since the active power is the orthogonal projection of the complex power on real axis.

2.3. Analysis of PQ variation method

2.3.1 Fundamentals

The ideal behavior of (the *Phase Locked Loop* of) the inverter is obtained by generating a grid current that is *at any instant* equal to the reference current. By this way, it is not necessary to implement a current controller, since at any instant the error between the reference and the grid current is zero**.**

The following scheme reproduces an ideal operation of the system without considering the blocks related the measurement and estimation operations:

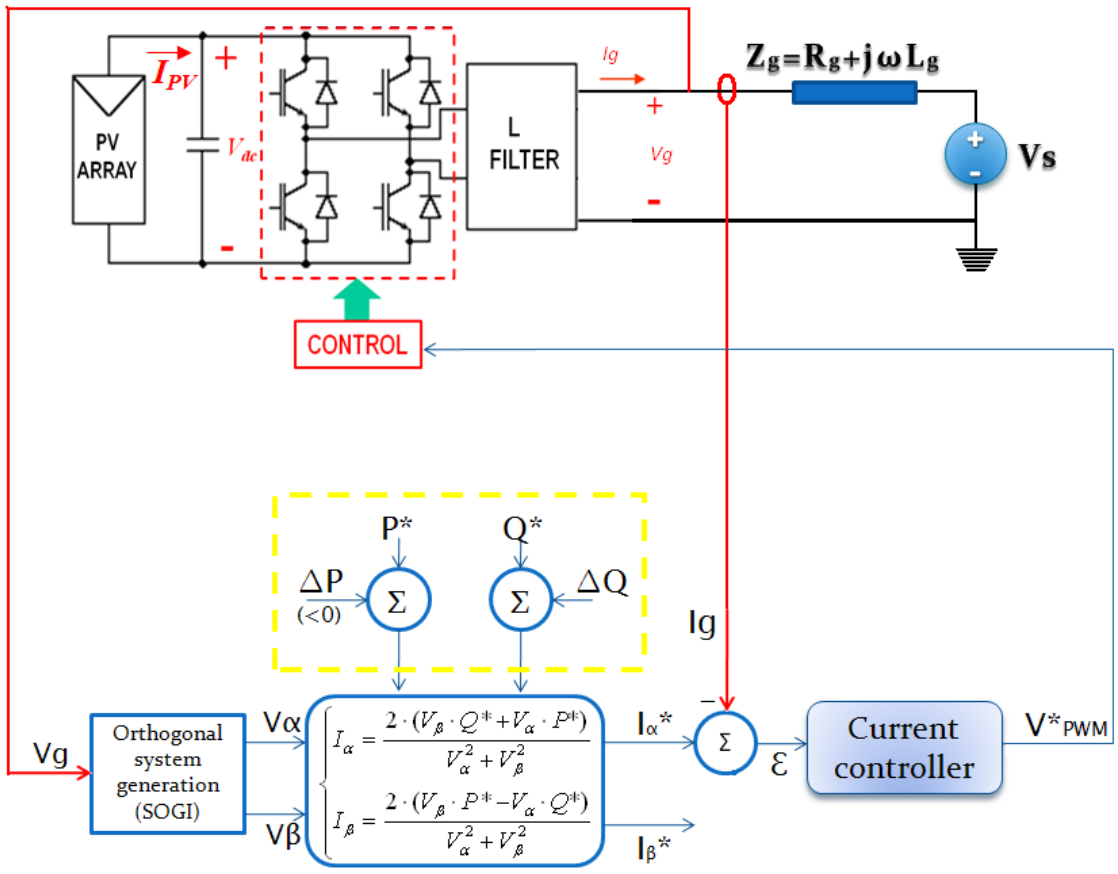

Fig. 1.5: The complete single-phase system

The grid-side voltage Vs is a sinusoidal voltage source and it has been used as a "source" for this simplified model: in fact, the voltage at the PCC depends not only by grid impedance Zg but also by Vs.

The inputs to the system are the reference active and reactive power values (P* and Q*) and the voltage source Vs. The values P* and Q* are constant and they define the reference working point of the inverter. The reference active power is less or equal to the maximum power delivered by local source (i.e. PV panels). Generally, the maximum amount of active power is detected tracking the output characteristic of the renewable source through a Maximum Power Point (MPP) device. The reference reactive power Q* is obviously zero.

The PQ variation method proposed by Ciobotaru *et al.* is based on the "p-q Theory" applied to the single-phase systems, but it uses a quite different matrix respect to Akagy in order to calculate the powers (notice that the Q has opposite sign):

$$\begin{bmatrix} P \\ Q \end{bmatrix} = \frac{1}{2}\begin{bmatrix} V_\alpha & V_\beta \\ V_\beta & -V_\alpha \end{bmatrix}\begin{bmatrix} I_\alpha \\ I_\beta \end{bmatrix} \tag{1.30}$$

where $V_\alpha, V_\beta, I_\alpha, I_\beta$ are the components of grid voltage and current respectively in the αβ stationary frame.

By inverting this matrix or by substitution, since V_α and V_β are known and P* and Q* are the reference power values, the current reference waveforms in the stationary frame can be calculated:

$$\begin{bmatrix} P \\ Q \end{bmatrix} = \frac{1}{2}\begin{bmatrix} V_\alpha & V_\beta \\ V_\beta & -V_\alpha \end{bmatrix}\begin{bmatrix} I_\alpha \\ I_\beta \end{bmatrix} \tag{1.32}$$

$$\Rightarrow \quad \begin{bmatrix} I_\alpha \\ I_\beta \end{bmatrix} = \frac{1}{\Delta}\begin{bmatrix} -V_\alpha & -V_\beta \\ -V_\beta & V_\alpha \end{bmatrix}\begin{bmatrix} P^* \\ \end{bmatrix} \tag{1.31}$$

where $\Delta = -\frac{2}{V_\alpha^2 + V_\beta^2}$.

The calculated reference currents in the stationary frame are:

$$\begin{cases} I_\alpha^* = \dfrac{2(V_\alpha \cdot P^* + V_\beta \cdot Q^*)}{V_\alpha^2 + V_\beta^2} \\ I_\beta^* = \dfrac{2(V_\beta \cdot P^* - V_\alpha \cdot Q^*)}{V_\alpha^2 + V_\beta^2} \end{cases} \tag{1.33}$$

that are different respect to the eq. 1.15 since here Q* has an opposite sign.

Since only one phase exists, the β current component is neglected and I_α^* is used as reference current. Both the current components are sinusoidal waveforms with the same amplitude but 90º degrees shifted: any change in P* or Q* affects both these components.

2.3.2. Estimation requirements: orthogonal voltages generation

The V_α and V_β voltages are obtained using an orthogonal system generator by measuring the amplitude and the phase of the voltage at PCC.

Ciobotaru *et al.* proposed to use a Second Order Generic Integrator – Single Signal Integrator (SOGI - SSI).

The scheme of the SOGI is shown in the following figure:

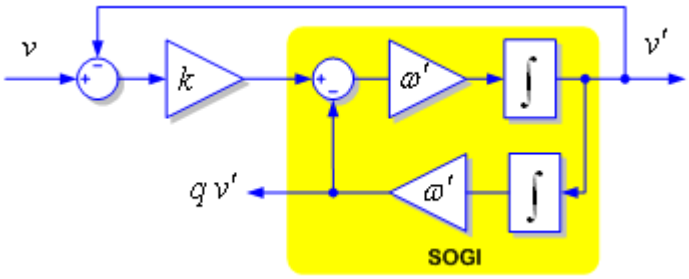

Fig. 1.6: the SOGI-SSI system

It' mandatory to use a second order system since a precise phase shift at a certain frequency is required.

The transfer functions of the SOGI are defined:

$$\begin{cases} D(s) = \dfrac{V\alpha}{Vg(s)} = \dfrac{K\omega' s}{s^2 + K\omega' s + \omega'^2} \\ Q(s) = \dfrac{V\beta}{Vg}(s) = \dfrac{K\omega'^2}{s^2 + K\omega' s + \omega'^2} \end{cases} \tag{1.34}$$

$$D(s) = \begin{cases} |D| = \dfrac{K\omega'\omega}{\sqrt{(K\omega'\omega)^2 + (\omega^2 - \omega'^2)^2}} \\ Phase\ of\ D(s) = \tan^{-1}\dfrac{\omega'^2 - \omega^2}{K\omega'\omega} \end{cases} \tag{1.35}$$

$$Q(s) = \begin{cases} |Q| = \dfrac{\omega'}{\omega|D|} \\ Phase\ of\ Q(s) = phase\ of\ D(s) - \dfrac{\pi}{2} \end{cases} \tag{1.36}$$

Referring to the input signal again, the v' voltage is the output of a band pass filter and qv' is the output of the cascade of low pass and band pass filters. The voltages v' and qv' (where q is the ratio between the center frequency ω' of SOGI and grid frequency ω) are Vα and Vβ respectively. The center frequency must be equal to the grid frequency 2π·50 rad/s. The value of ω' affects both the amplitude and the phase of V_α and V_β. The gain K defines the selectivity of the SOGI filter itself. A narrow bandwidth of the SOGI id defined from a K value below unity.

The Bode plots of the SOGI-SSI are shown in the figure 1.7, for K=0.8:

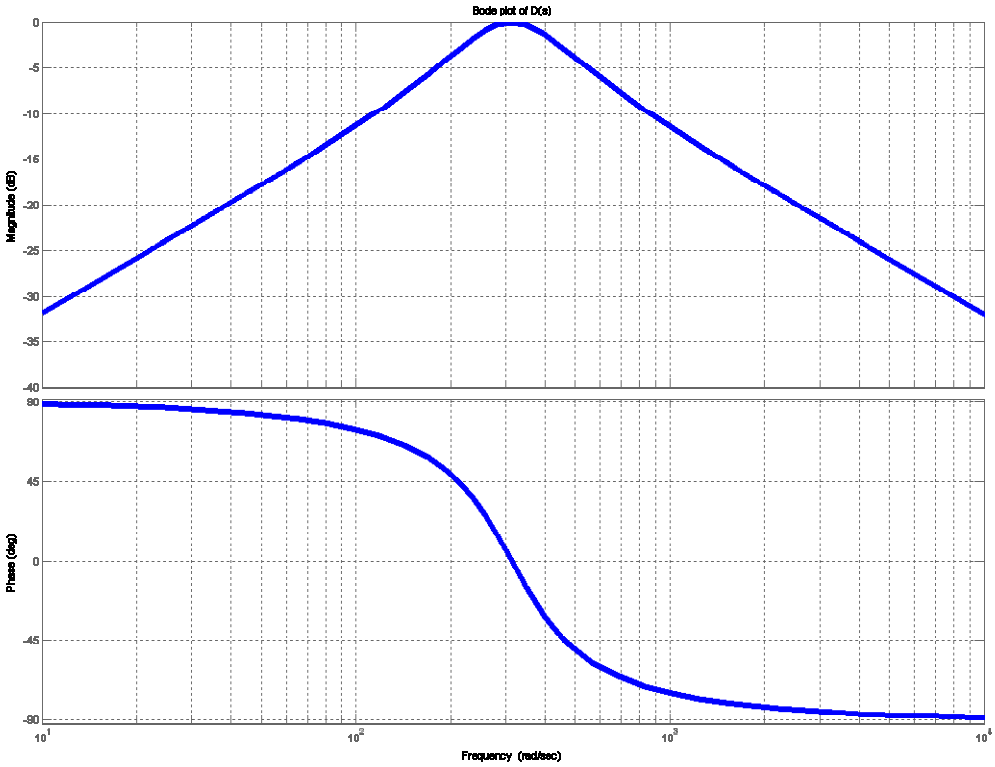

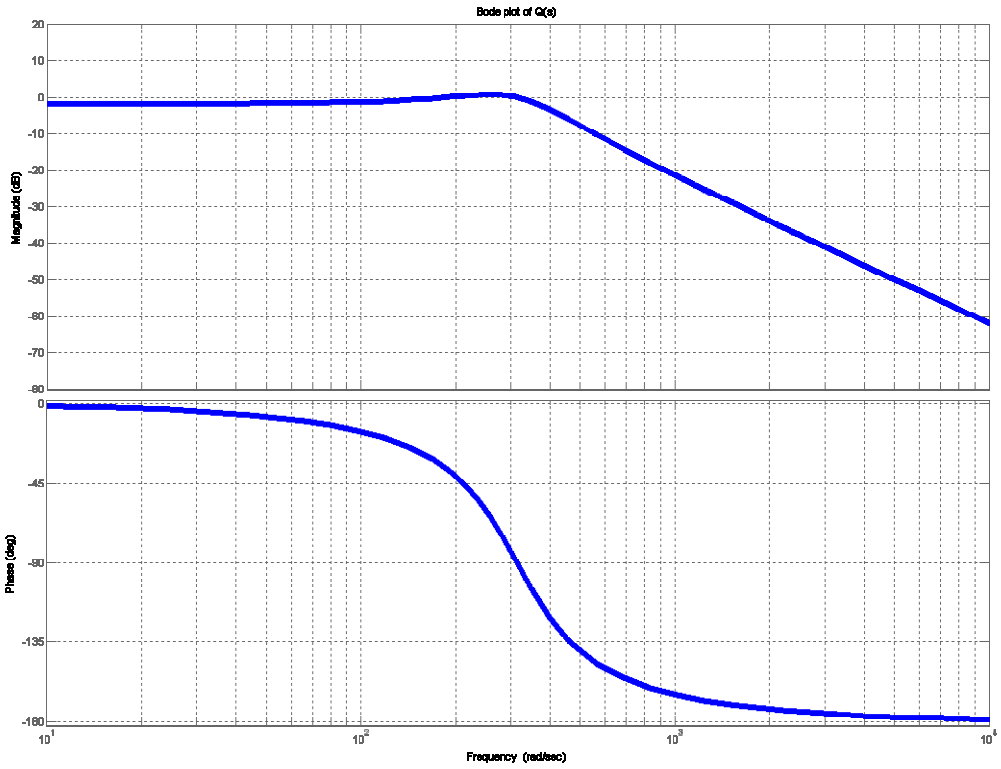

Fig. 1.7: the bode plot of the SOGI filter

2.3.2. Estimation requirements: grid-side voltage influence

As mentioned, the proposed estimation technique is based on active and reactive power variation. Once the system is stable, the active (or reactive) power is changed by a fixed amount ΔP (or ΔQ) and the resistance (or the inductance) is estimated by evaluating the voltage and current variation at the PCC. The most relevant aspect is that the value of the grid-side voltage is not important, but it must not change during all measurement period.

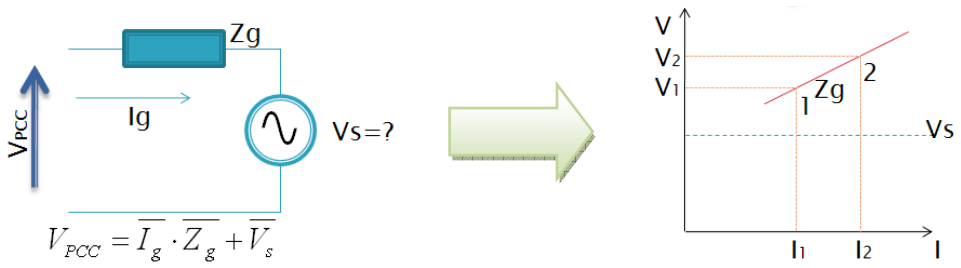

Fig. 1.8: the graphical interpretation of the PQ variation method.

The grid impedance is estimated as ratio between the voltage and current variation phasors.

$$Z_g = \frac{\overline{V_2} - \overline{V_1}}{\overline{I_2} - \overline{I_1}} = R_g + jX_g \qquad (1.37)$$

As can be noticed, the grid-side voltage value is not involved in the estimation phase if it doesn't change (the dotted blue line in the figure remains at a constant level).

2.3.2. Estimation requirements: synchronous frame reference

It's difficult to estimate the grid impedance by measuring the grid current and voltage in the stationary reference frame since, in this case, both amplitude and phase should be measured in order to make correctly a phasor subtraction.

Indeed, a synchronous frame reference can be built over the stationary reference frame: this reference frame is rotating at grid frequency and it has the same phase of grid voltage V_g.

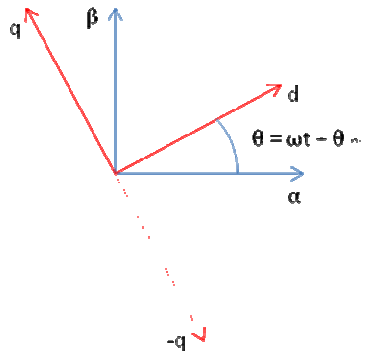

Fig. 1.9: the stationary and synchronous reference frame

The transformation from the αβ stationary frame to the dq rotating synchronous frame is called *Park Transformation.*

The d and q components are calculated by Park transformation matrix:

$$\begin{bmatrix} d \\ q \end{bmatrix} = \begin{bmatrix} \cos\theta & \sin\theta \\ -\sin\theta & \cos\theta \end{bmatrix} \begin{bmatrix} \alpha \\ \beta \end{bmatrix} \qquad (1.38)$$

It should be important to remember that the reactive power is taken with an opposite sign to the original Akagy's Theory. So, in order to have the same plots of the reference paper, the –q axis is considered instead of q axis in Park transformation.

By this way, all variables are referred to the grid voltage phase: the θ angle is the phase difference between grid voltage Vg and α axis taken as reference. Obviously, since the grid current and the grid voltage have the same phase, in this case only the d component should have a steady state value greater than zero. In fact, the q component can be considered a kind of "error" measure.

The components on d and q axis for the grid voltage and the grid current at steady state can be evaluated.

The grid voltage Vg in the stationary frame is:

$$\begin{cases} V_\alpha = V_g \cos(\omega t + \theta_g) \\ V_\beta = V_g \sin(\omega t + \theta_g) \end{cases} \tag{1.39}$$

and inversely

$$V_g = \sqrt{V_\alpha^2 + V_\beta^2} \tag{1.40}$$

$$\theta_g = \tan^{-1}\frac{V_\beta}{V_\alpha} \tag{1.41}$$

Using the Park transformation, the grid voltage stationary components become:

$$\begin{bmatrix} V_d \\ V_q \end{bmatrix} = \begin{bmatrix} \cos\theta & \sin\theta \\ -\sin\theta & \cos\theta \end{bmatrix} \begin{bmatrix} V_\alpha \\ V_\beta \end{bmatrix} = \begin{bmatrix} \cos\theta & \sin\theta \\ -\sin\theta & \cos\theta \end{bmatrix} \begin{bmatrix} V_g \cos(\omega t + \theta_g) \\ V_g \sin(\omega t + \theta_g) \end{bmatrix} = \begin{bmatrix} V_g \cos(\theta_g - \theta) \\ V_g \sin(\theta_g - \theta) \end{bmatrix} \tag{1.42}$$

Obviously if θ=θg, then Vd=Vg and Vq=0.

In a similar way for the grid current Ig, calling i_g the generic current amplitude:

$$\begin{cases} I_\alpha^* = \dfrac{2(V_\alpha P^* + V_\beta Q^*)}{V_{\alpha\beta}^2} \\ I_\beta^* = \dfrac{2(V_\beta P^* - V_\alpha Q^*)}{V_{\alpha\beta}^2} \end{cases} \tag{1.43}$$

$$\begin{bmatrix} i_d \\ i_q \end{bmatrix} = \begin{bmatrix} \cos\theta & \sin\theta \\ -\sin\theta & \cos\theta \end{bmatrix} \begin{bmatrix} i_\alpha^* \\ i_\beta^* \end{bmatrix} = \begin{bmatrix} \cos\theta & \sin\theta \\ -\sin\theta & \cos\theta \end{bmatrix} \begin{bmatrix} i_g \cos(\omega t + \theta_g) \\ i_g \sin(\omega t + \theta_g) \end{bmatrix} = \begin{bmatrix} i_g \cos(\theta_g - \theta) \\ i_g \sin(\theta_g - \theta) \end{bmatrix} \tag{1.44}$$

and, at the same time, substituting V_α and V_β in I_α^* and I_β^* formulas, it can be demonstrated that i_d depends only on active power and i_q depends only on reactive power. In fact:

$$i_d = i_\alpha^* \cos\theta + i_\beta^* \sin\theta \tag{1.45}$$

$$i_d = \frac{2}{V_g}[P^* \cos\theta + Q^* \sin\theta]\cos\theta + [P^* \sin\theta - Q^* \cos\theta]\sin\theta \tag{1.46}$$

$$i_d = \frac{2}{V_g}\left[P^*[(\cos]\theta)^2 + P^*(\sin\theta)^2\right] + [Q^* \sin\theta\cos\theta - Q^* \cos\theta\sin\theta] = \frac{2P^*}{V_g} \tag{1.47}$$

and, in a similar way for i_q:

$$i_q = -\frac{2}{V_g}[P^* \cos\theta + Q^* \sin\theta]\sin\theta + [P^* \sin\theta - Q^* \cos\theta]\cos\theta = -\frac{2Q^*}{V_g} \tag{1.48}$$

Since –q axis is considered, then $-v_q$ and $-i_q$ values must be considered.

If both the active and the reactive power are changed together, the grid impedance estimation is difficult to obtain since it could not be easy to well distinguish the P and Q effects. Instead, by changing one reference power for time, the single grid impedance components can be easily estimated.

By power theory, the resistive component influences only the active power and the reactance influences only the reactive power. This means it's possible to write also power variations in terms of Rg and Xg and that these quantities should be evaluated independently by P and Q variations respectively.

So:

$$\Delta P = Rg \left|\overline{\Delta I}\right|^2 \tag{1.49}$$

$$\Delta Q = Xg \left|\overline{\Delta I}\right|^2 \tag{1.50}$$

So the complex power S can be represented as a vector in the complex plane and the power variation components are written as:

$$\Delta P = Re(\Delta S) \tag{1.51}$$

$$\Delta Q = Im(\Delta S) \tag{1.52}$$

It can be demonstrated that is also $\Delta S = \overline{\Delta V}\ \overline{\Delta I}^*$, where the grid voltage and current are referred to the rotating frame. So these variables are seen as vectors with a direct and a quadrature component.

Indeed, the following plot shows the complex power variation:

$$\Delta S = V_1 I_1^* - V_2 I_2^* = \left(\overline{V_2}\ \overline{I_2^*} + \overline{\Delta V}\ \overline{\Delta I}^*\right) - \overline{V_2}\ \overline{I_2^*} = \overline{\Delta V}\ \overline{\Delta I}^* \tag{1.53}$$

Therefore:

$$\Delta P = Re\left(\overline{\Delta V}\ \overline{\Delta I}^*\right) \tag{1.54}$$

$$\Delta Q = Im\left(\overline{\Delta V}\ \overline{\Delta I}^*\right) \tag{1.55}$$

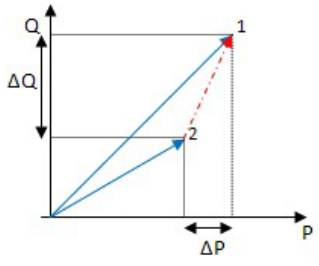

Fig. 1.10: the vector representation of the complex power variation

Substituting $\overline{\Delta V} = \Delta V_d + j\Delta V_q$ and $\overline{\Delta I} = \Delta I_d + j\Delta I_q$, then:

$$\Delta P = Re\left(\overline{\Delta V}\ \overline{\Delta I}^{*}\right) = Re\left(\left(\Delta V_d + j\Delta V_q\right)\left[\left(\Delta I\right]_d - j\Delta I_q\right)\right) = \Delta V_d \Delta I_d + \Delta V_q \Delta I_q \quad (1.56)$$

$$\Delta Q = Im\left(\overline{\Delta V}\ \overline{\Delta I}^{*}\right) = Im\left(\left(\Delta V_d + j\Delta V_q\right)\left[\left(\Delta I\right]_d - j\Delta I_q\right)\right) = \Delta V_q \Delta I_d - \Delta V_d \Delta I_q \quad (1.57)$$

Remembering the equations [1.49] and [1.50], the R_g and X_g formulas are obtained:

$$\begin{cases} Rg = \dfrac{\Delta V_d \Delta I_d + \Delta V_q \Delta I_q}{\Delta I_d^{\,2} + \Delta I_q^{\,2}} \\ Lg = \dfrac{1}{\omega} \dfrac{\Delta V_q \Delta I_d - \Delta V_d \Delta I_q}{\Delta I_d^{\,2} + \Delta I_q^{\,2}} \end{cases} \quad (1.58)$$

The grid resistance and reactance are evaluated as ratio between the measured power variation (active for Rg and reactive for X_g) and the grid current squared.

The active power variation ideally affects only the direct component since the quadrature component don't depend on it, and, vice versa, the reactive power variation should affect only the quadrature components. In order to have optimal impedance estimation and to be very near to the ideal case, the system must reach the steady state after any power perturbation.

Chapter 2

A Simulink-Based approach to the PQ Variation Method

2.1.Introduction

In the previous chapter, the proposed grid impedance estimation technique has been analyzed. Previously, the method has been studied in a very ideal scenario: in fact, instant by instant the equality between the grid current and the reference current has been hypothesized.

Instead, in this chapter the proposed method has been implemented in a more realistic scenario; in fact, the following elements are introduced:

- A real PV array model
- A DC-link capacitor with a big value (2.2mF)
- An ideal full bridge DC/AC inverter
- A simple inductance as *output filter*
- A proportional resonant filter as *current controller*
- An unipolar pulse with modulator (unipolar PWM)

The figure 2.1 shows the complete system:

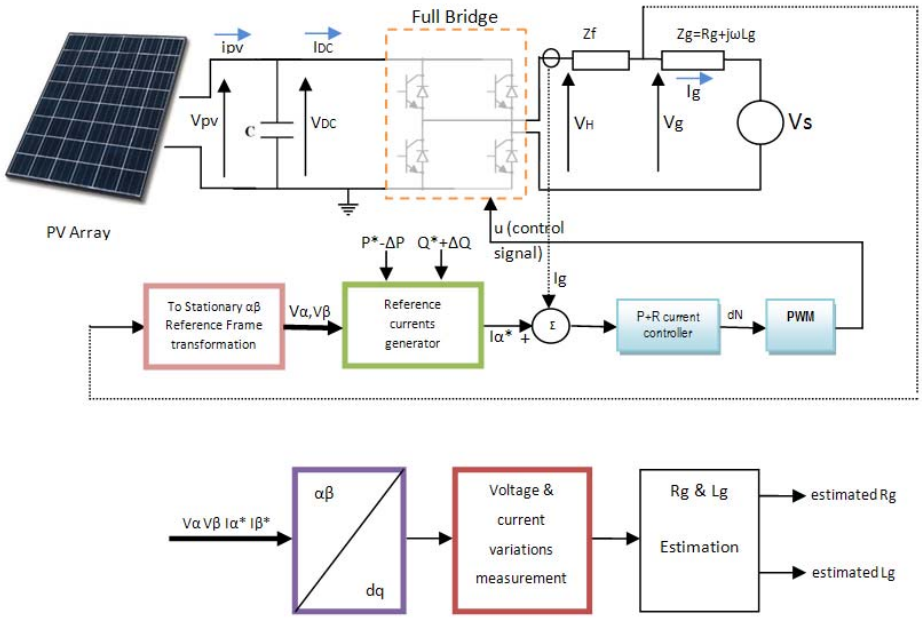

Fig. 2.1 The complete single-phase system with the measurement and estimation blocks

The complete system could be seen as divided into two parts (a power and a measurement sub-system): the former is related to the power elements connected to the grid; the latter, instead, is composed by all elements that are involved into the measurement and processing of both grid current and voltage and into the estimation of grid impedance.

The modification of the power sub-system, through the introduction of the new elements (such as the current controller), affects the response time of the full system. The value of DC capacitor affects the initialization time and the time response of the system too, but, at the same time, using a great value of the capacitance, the photovoltaic voltage oscillations (around the average active power value) are reduced. No delay is introduced by measurement and estimation blocks.

It is always necessary to wait that the system stabilizes itself after every single power perturbation. Furthermore, it's a good idea to take the reference values always before every power perturbation, since V_s could be changed after the previous impedance component estimation.

In the following, the implemented Matlab®/Simulink system will be described.

2.2. The photovoltaic array

The first important difference with the previous analysis of the proposed method is the implementation of a *real* photovoltaic array model as power source of the full system.

The photovoltaic module is composed by a matrix of solar cells. The single solar cell model is represented by the following circuit:

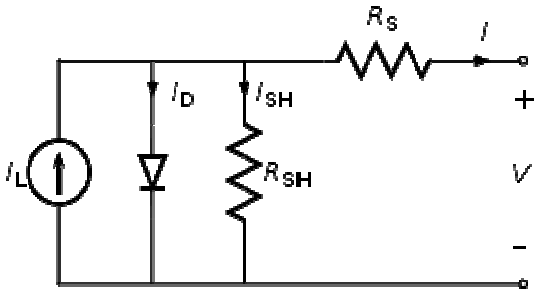

Fig. 2.2 The photovoltaic cell model

where:

- *IL or Igc* is the photocurrent generated by the incident light, directly proportional to the sun irradiation (and the cell area).
- *ID* is the current diode
- *Rsh* and *Rs* are respectively the shunt and series resistances.
- *Ish* is the current through the shunt resistor.
- *V* is the PV cell voltage

The single PV cell current *I* is given by the following equation:

$$I = I_{gc} - I_{satc}\left(e^{\frac{V+IR_s}{\eta V_T}} - 1\right) - \frac{V + IR_s}{R_{sh}} \qquad (2.1)$$

where $V_T = \frac{kT}{q}$ (2.2) is the thermal voltage and $I_{satc} = I_{sato}\left(\frac{T}{T1}\right)^{\frac{3}{\eta}} e^{\frac{qV_{gap}(T1)}{\eta k\left(\frac{1}{T}-\frac{1}{T1}\right)}}$ (2.3) is the saturation current of the diode at the temperature T.

Moreover:

- T is the current cell temperature in Kelvin
- T1 is the reference temperature equal to 298K
- η is the ideality factor of the diode
- k is the Boltzmann's constant (k=1.38*10^-23 [J/K])

- q is the charge of the electron (q=1.6*10^-19 Coulomb)
- Isat0 is the saturation current of the diode at the reference temperature T1

Isat0 can be calculated as $$I_{sat0} = \frac{I_{sc}(T1)}{\left(e^{\frac{q\,V_{OC}(T1)}{\eta\,k\,T1}} - 1\right)}.$$ (2.4)

The most important parameters for the PV cell are:

- The short circuit current *Ish*=Igc; it is the highest value of current generated by the PV cell.
- The open circuit voltage corresponds to the voltage drop across the diode (p-n) junction when it is traversed by the photocurrent I_L.

  It is mathematically expressed as $$V_{OC} = V_t ln\left(\frac{I_{gc}}{I_{sat0}}\right).$$ (2.5)
- The maximum power point is the operating point (V_{max}, I_{max}) at which the power dissipated in the load resistance is maximum.
- The maximum efficiency is the ratio between the maximum power and the incident light power.
- The fill factor is the ratio between the maximum power that can be delivered to the load and the product between V_{oc} and I_{sc}..

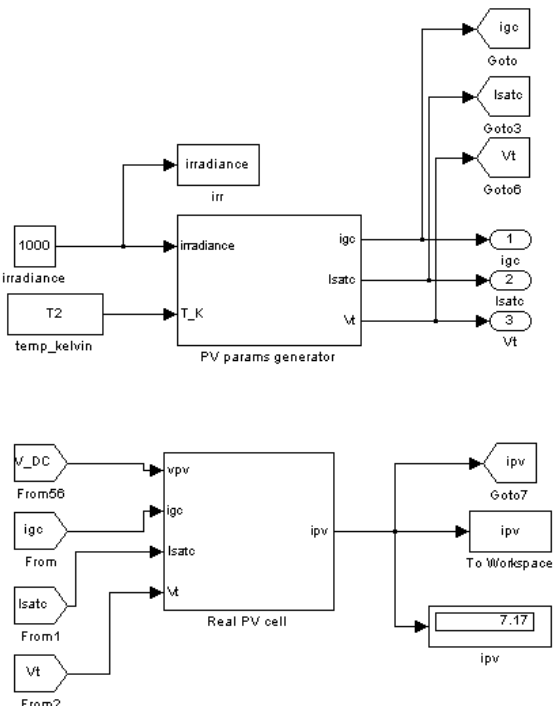

Fig. 2.3: The photovoltaic cell blocks

The implemented PV cell model is composed by two blocks, but in effect all can be seen as a unique block, whose inputs are the irradiance and temperature and the output is the photovoltaic current.

The first step is to calculate the photo generated current, the saturation current of the diode and the thermal voltage from irradiance and temperature values.

Once these values are estimated, the i_{pv} current is calculated by solving the node equation of the cell model.

The following figure show more in detail the blocks.

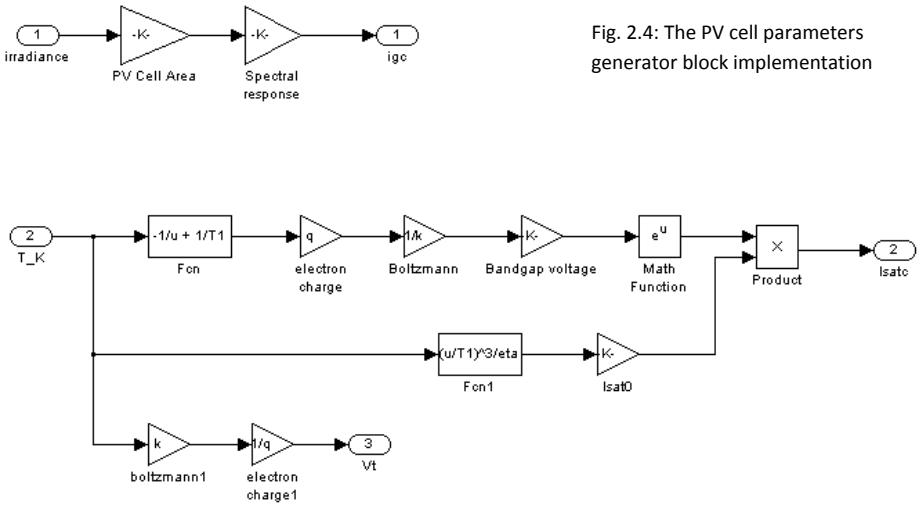

Fig. 2.4: The PV cell parameters generator block implementation

The photo generated current *igc* depends by the area of the photovoltaic cell and by the spectral response (the amount of light spectrum a single cell is able to absorb).

The temperature value affects the saturation current of the diode and the thermal voltage.

The i_{pv} value is affected also by shunt and series resistance values, since the real PV cell has been implemented.

Fig. 2.4: The ipv generation block implementation

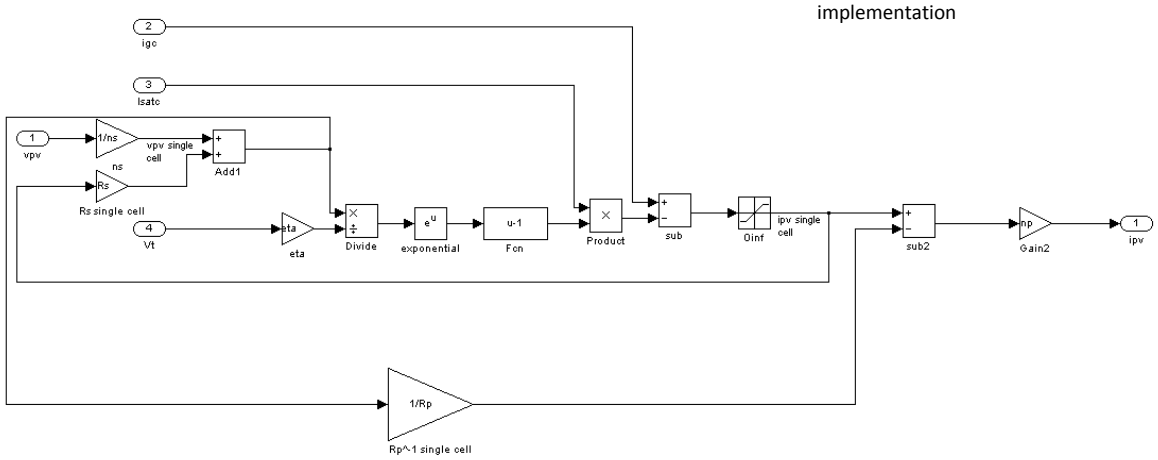

All the parameters are used for a single cell and then, considering all equal cells, the i_{pv} value is estimated as product of the i_{pv} of a single cell and the number of the parallel cells n_p. Instead, the photovoltaic voltage is divided by the number of cells in series n_s.

The output characteristics and the output power of the cell are shown in the fig. 2.5 and 2.6:

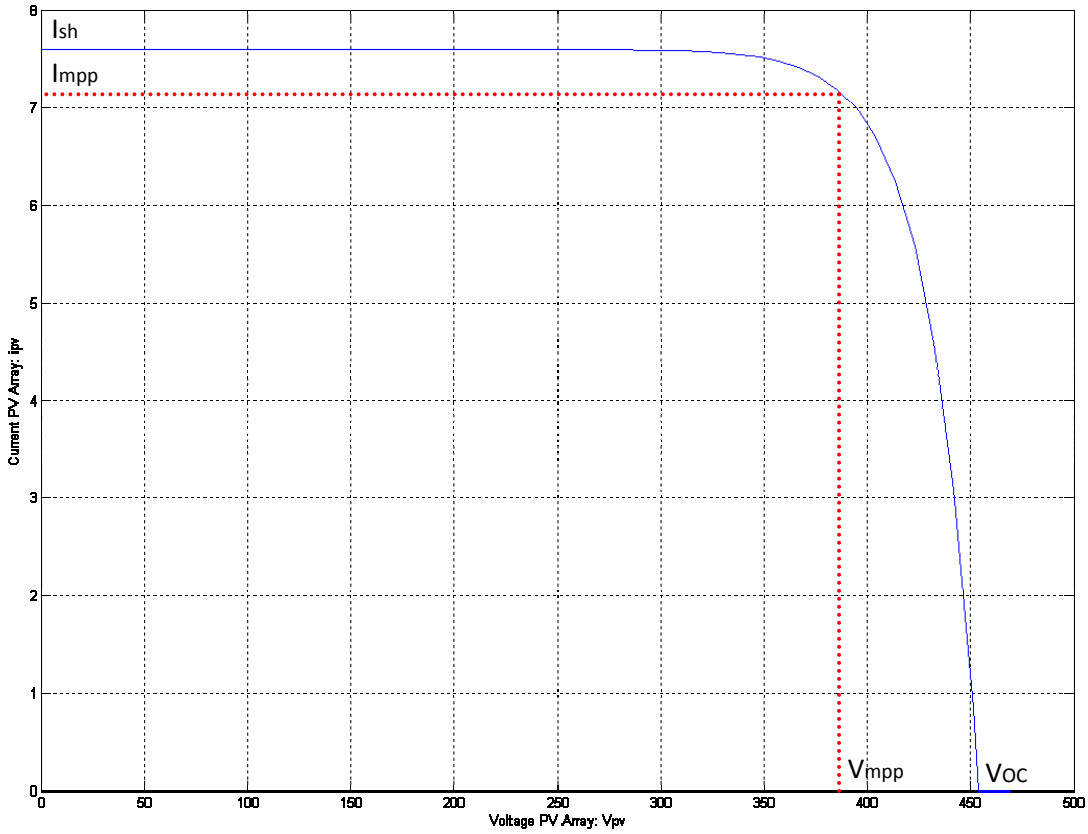

Fig. 2.5: The PV array output characteristic: ipv current VS voltage array

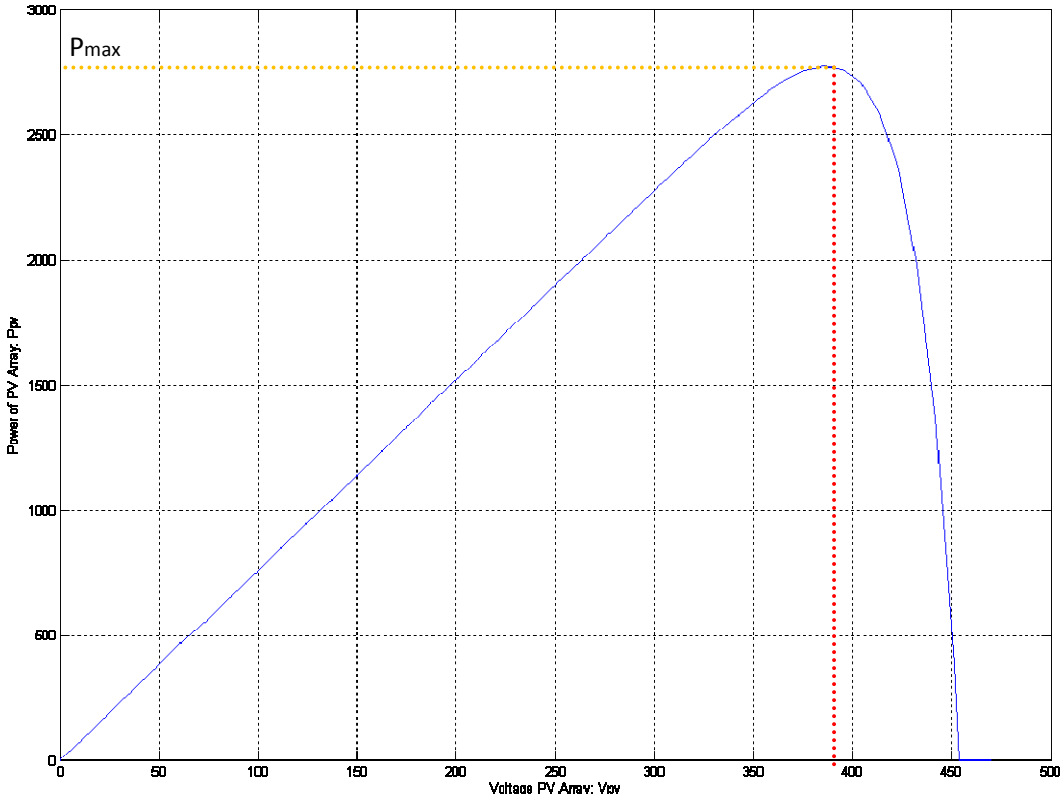

Fig. 2.6: The PV array output characteristic: PV power VS voltage array

The table 2.1 shows the parameters of the photovoltaic module:

Maximum Power [Watt]	2773.6 Watt
Voltage at maximum power Vmpp	390V
Current at maximum power Impp	7.1A
Open circuit voltage VOC	453.9V
Short circuit current Ish	7.6A
Fill Factor	0.8

Table 2.1: PV array parameters

In order to reduce the oscillations of the DC-link capacitor voltage, a reference active power near the maximum value should be chosen.

2.3.The Full Bridge inverter

The model of the full bridge inverter can be derived considering that its input voltage is the capacitor voltage and that the output current is the filter inductor current (and the grid current) and that these variables depend on control signal u(t).

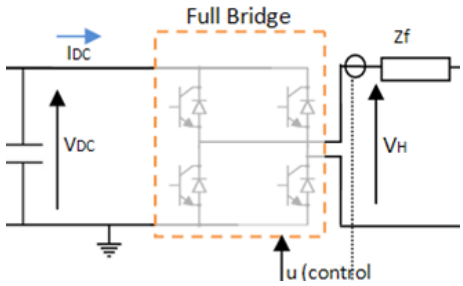

Fig. 2.7: The inverter block

The inverter equations can be found starting from the state equations:

$$\begin{cases} V_{Lf} = L_f \dfrac{d(i_{Lf})}{dt} \\ i_C = C \dfrac{d(v_{DC})}{dt} \end{cases} \tag{2.6}$$

since the filter is just an L_f series inductance.

Analyzing the circuit model, it is possible to proof the following equations about the state variables:

$$\begin{cases} V_{Lf} = V_H - V_g = u * V_{DC} - V_g \\ i_C = i_{pv} - u * i_{Lf} \end{cases} \tag{2.7}$$

where u=u(t) is the signal that define which mosfets are on/off.

Before proofing the previous equations, it is worth to stress that they are valid both in a switched and in an averaged model of the inverter. So, independently of the used model, the equations are always valid but the meaning of the control signal u(t) is different.

Two different kinds of models have been considered to calculate the output voltage of the full bridge inverter: a switched and an averaged model. The main difference is focused on how the control signal u(t) is calculated: in the switched model of the inverter, the control signal u(t) is the output of the pulse with modulator and it can assume only three discrete values (-1, 0, 1). The value of u(t) depends on the normalized duty signal, which is the output of the current controller; in the averaged model, u(t) is a continuous signal given by filtering the normalized duty signal (respect to V_{dc}) through a saturation block (with a unitary gain between -1 and +1). In the averaged model the signal u(t) is a normalized sinusoidal waveform whose frequency is defined by the central frequency of the current controller (50Hz). So, the only difference is that, in the averaged version of the inverter, the PWM block is simply replaced by a saturation block.

In order to proof the previous equations by analyzing the behavior of the inverter respect to the control signal u(t), the switched version of the inverter is considered:

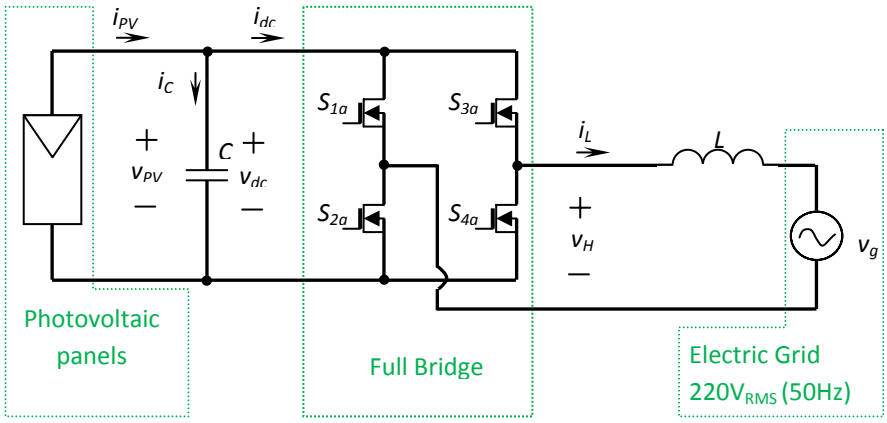

Fig. 2.8: The switched inverter general scheme

The table 2.2 summarizes the values assumed by the control signal u(t) in order to switch on/off the inverter mosfets:

u	S_1	S_2	S_3	S_4	V_H
1	OFF	ON	ON	OFF	$+v_{PV}$
0	ON	OFF	ON	OFF	0
0	OFF	ON	OFF	ON	0
-1	ON	OFF	OFF	ON	$-v_{PV}$

Table 2.2: the relationship between the control variable u and the switching of mosfets

Starting from this table, it's clear that four state of inverter exist:

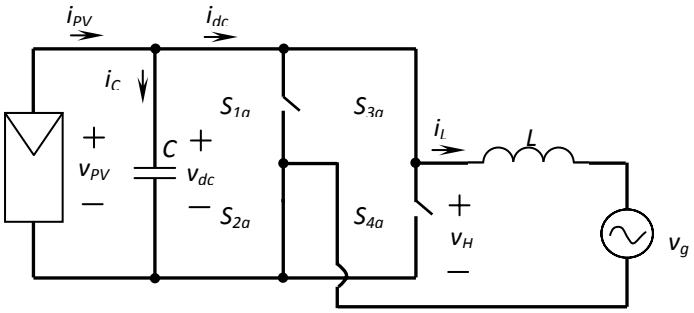

$$\left.\begin{aligned} v_{Lf} &= L\cdot\frac{di_L}{dt} = v_H - v_g = v_{dc} - v_g \\ i_C &= C\cdot\frac{dv_{dc}}{dt} = i_{pv} - i_{dc} = i_{pv} - i_L \end{aligned}\right\}$$

Fig 2.9.a: State of the inverter when u=1 with equations (2.8)

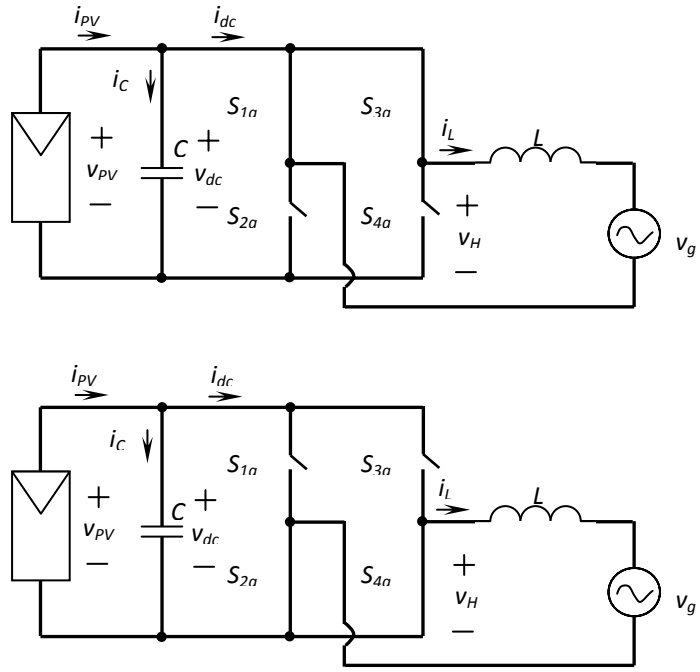

$$\left.\begin{aligned} v_{Lf} &= L\cdot\frac{di_{Lf}}{dt} = v_H - v_g = -v_g \\ i_C &= C\cdot\frac{dv_{dc}}{dt} = i_{pv} - i_{dc} = i_{pv} \end{aligned}\right\}$$

Fig 2.9.b: State of the inverter when u=0 with equations (2.9)

When the u signal is equal to zero the input and the output of the full bridge are decoupled.

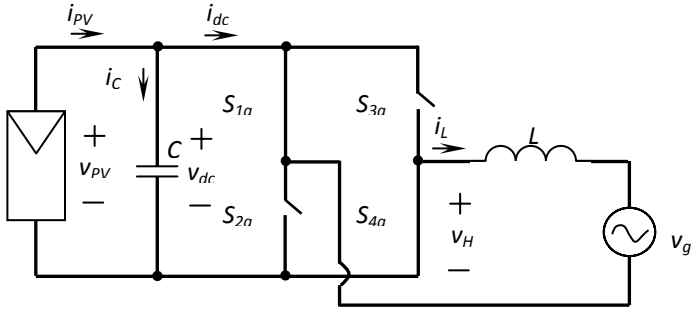

$$\left.\begin{aligned} v_L &= L\cdot\frac{di_L}{dt} = v_H - v_g = -v_{dc} - v_g \\ i_C &= C\cdot\frac{dv_{dc}}{dt} = i_{pv} - i_{dc} = i_{pv} + i_{Lf} \end{aligned}\right\}$$

Fig 2.9.c: State of the inverter when u=-1 with equations (2.10)

Putting all equations (2.8, 2.9 and 2.10) in a unique one the eq. 2.7 is retrieved:

$$\begin{cases} V_{Lf} = V_H - V_g = u * V_{DC} - V_g \\ i_C = i_{pv} - i_H = i_{pv} - u * i_{Lf} \end{cases} \quad (2.7)$$

and remembering the eq. 2.6, the following formulas are obtained and implemented in order to obtain the state variables i_g=i_{Lf} and the V_{DC} voltage of the DC-link capacitor:

$$i_{Lf} = \int \frac{V_{Lf}}{L_f} dt = \int \frac{u * v_{DC} - v_g}{L_f} dt \quad (2.11)$$

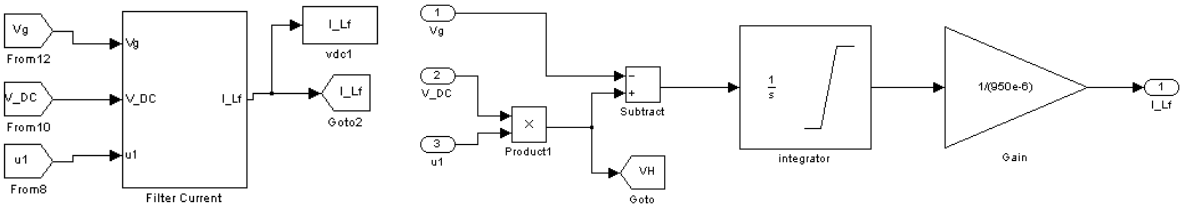

Fig. 2.10: The grid current "generator"

$$v_{DC} = \int \frac{i_C}{C_{DC}} dt = \int \frac{i_{pv} - u * i_{Lf}}{C_{DC}} dt \quad (2.12)$$

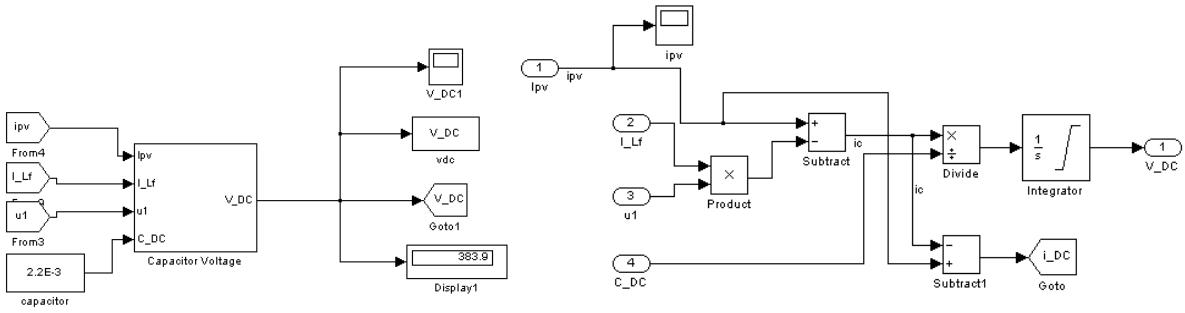

Fig. 2.11: The DC-link voltage "generator"

A big value of capacitance has been chosen (2.2mF) to ensure small variations of Vdc once the point of work has been established. The output filter is just an inductance L_f equal to 950µH.

2.4. The current controller

The current controller and the pulse width modulator are connected in cascade, as the fig. 2.12 shows.

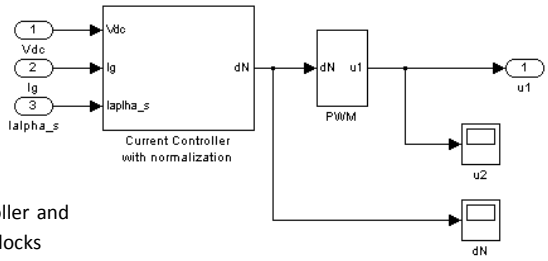

Fig. 2.12: The current controller and the Pulse Width Modulator blocks

The current controller is implemented by a proportional - resonant filter whose parameters (Kp, the proportional gain, and Ki, the integrator's gain) are chosen equals to 140 and 50000 respectively. The input signal of this filter is the error signal or the difference between the reference current I_α* and the grid current I_g.

The output is the so-called duty signal that is directly proportional to the error signal.

Since a normalized signal is needed as input to the pulse width modulator, the duty signal is divided by V_{dc}, returning the normalized duty signal d_N.

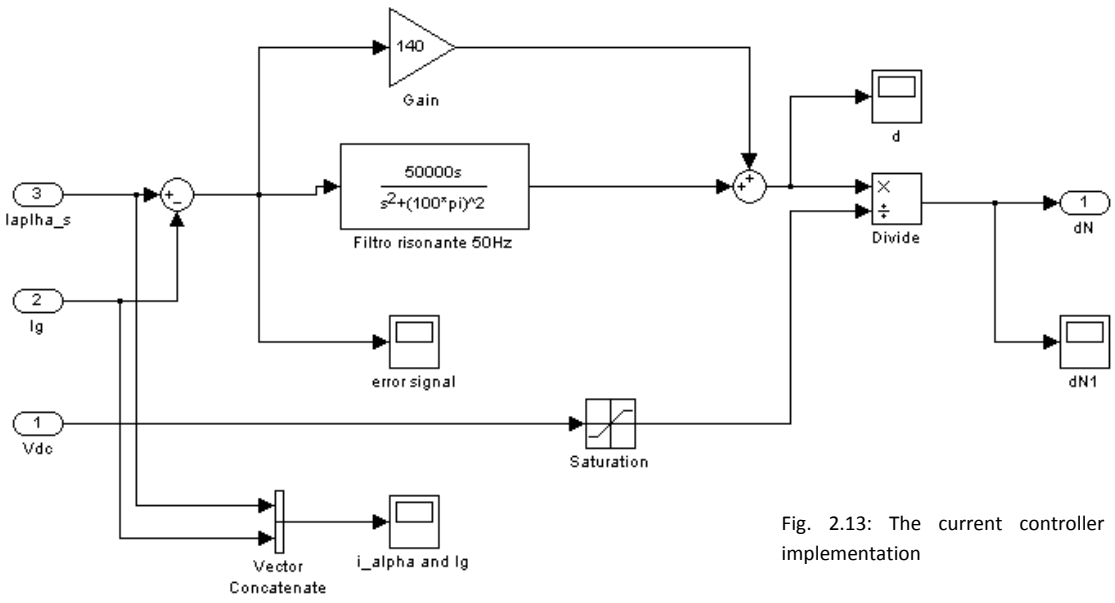

Fig. 2.13: The current controller implementation

A saturation block is needed to ensure that the taken V_{dc} value is always non negative.

2.5. The pulse width modulator

The pulse width modulator compares (by using a subtractive block) the input signal d_N (and its negative version) with a triangular carrier signal whose frequency is 10 kHz.

The output of the subtractive block is then compared with a zero threshold to get, if the input is a positive value, the unitary value or zero otherwise.

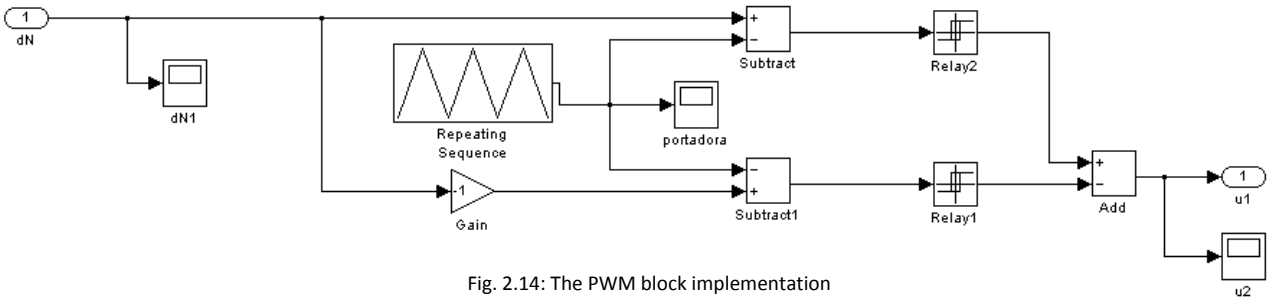

Fig. 2.14: The PWM block implementation

The discontinuous control signal u(t) is obtained as difference between the instantaneous values of the two relays.

2.6. The grid voltage Vg

As regards the grid voltage Vg, two scenarios have been analyzed during the implementation:

- The grid voltage is a pure sinusoidal signal independent of grid current value (no grid impedance has been considered)

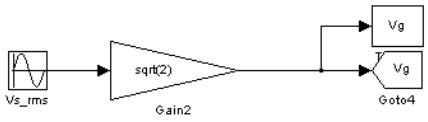

Fig. 2.15: the Vg "generator" without grid impedance

- A grid impedance is introduced and so the grid voltage depends on grid current value

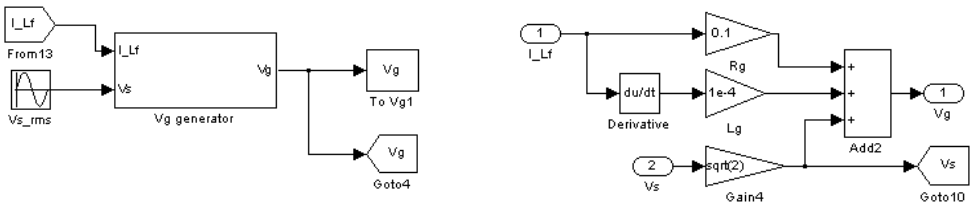

Fig. 2.16: the Vg "generator" with grid impedence

The first scenario has been considered in order to test the working of the current controller: in this case, the impedance estimation is senseless.

In the other case, the PQ Variation Method can be applied and the above circuit implements the Thévénin model of the grid. The grid voltage is the sum of 3 signals:

1. The grid-side voltage V_s. Notice that the input voltage V_s is an RMS value and for this reason this waveform is multiplied by the square root of two.
2. The resistance voltage drop; the resistance value is 100mΩ.
3. The inductive voltage drop; the inductance value is 100µH.

The effect of the grid inductance value could affect the grid voltage waveform if some disturb is present in the line. The chosen values are taken from the method's paper in order to be consistent with the author's method implementation.

2.7. The stationary frame reference current generator

The aim of this block is to generate a grid reference current I_α* by giving as inputs the reference active and reactive power values, their step variation given as pulse waveforms, the grid voltage V_g and an enabling signal in order to allow the impedance estimation only once the system has become stable.

It's worth to notice that the active power reference hasn't the required value at the beginning of the simulation but it is built as a high slope ramp until it reaches the final value P_{ref} (set in the saturation block) in order to reduce the initial reactive power oscillation.

The following figures show the block and its content: it is composed by the SOGI-SSI filter and the current reference generator in cascade.

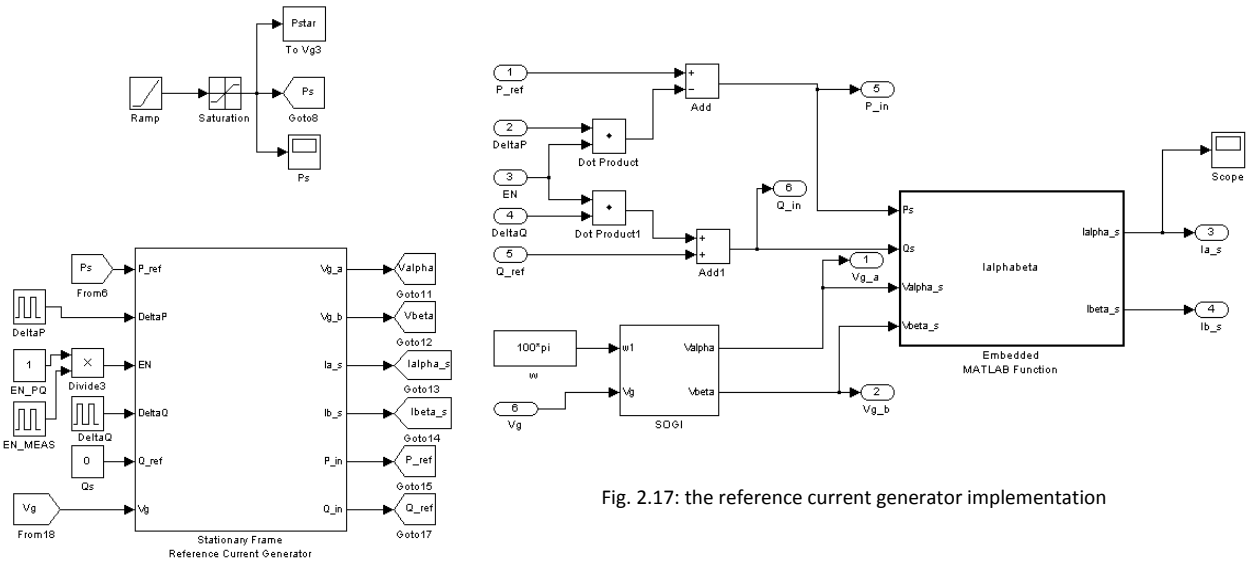

Fig. 2.17: the reference current generator implementation

As mentioned in the previous chapter, the reference current is generated by the following formula (since the system has only one phase the I_β^* current is neglected):

$$I_\alpha^* = \frac{2\left(V_\alpha \cdot P^* + V_\beta \cdot Q^*\right)}{V_\alpha^2 + V_\beta^2} \tag{2.13}$$

where P* and Q* include the step power variation during the measurement period. The stationary current components are generated through an embedded Matlab® function.

The voltage components V_α and V_β are the output of SOGI filter (see the figure 2.18).

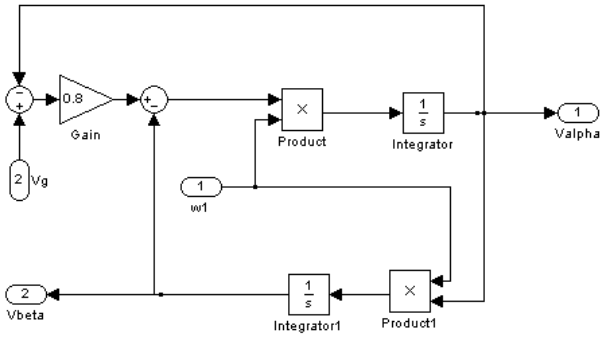

Fig. 2.18: the SOGI-SSI implementation

Furthermore, the power perturbation is managed by the enabling signal EN in order to guarantee that, during the simulation interval, only one estimation process takes place.

2.8.The synchronous frame reference generator

Once the voltage and current stationary components are generated, it's necessary to transform them into synchronous dq components, where the direct component has the same grid voltage phase and angular velocity.

These blocks are implemented through Embedded Matlab® functions.

The fig. 2.19 and 2.20 show the generation of matrix transformation components (cosine and sine):

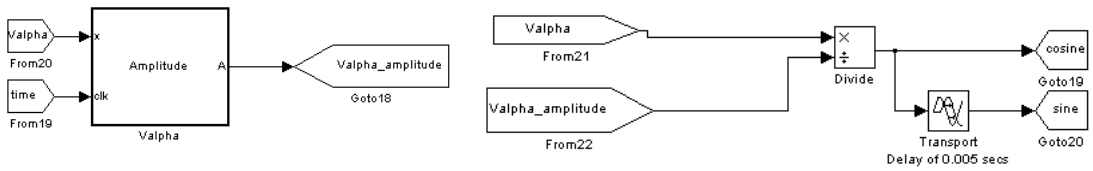

Fig. 2.19: a grid voltage normalizer

And the dq components generation blocks: the -1 gain is used in order to be consistent with authors' work as regards the q-components sign.

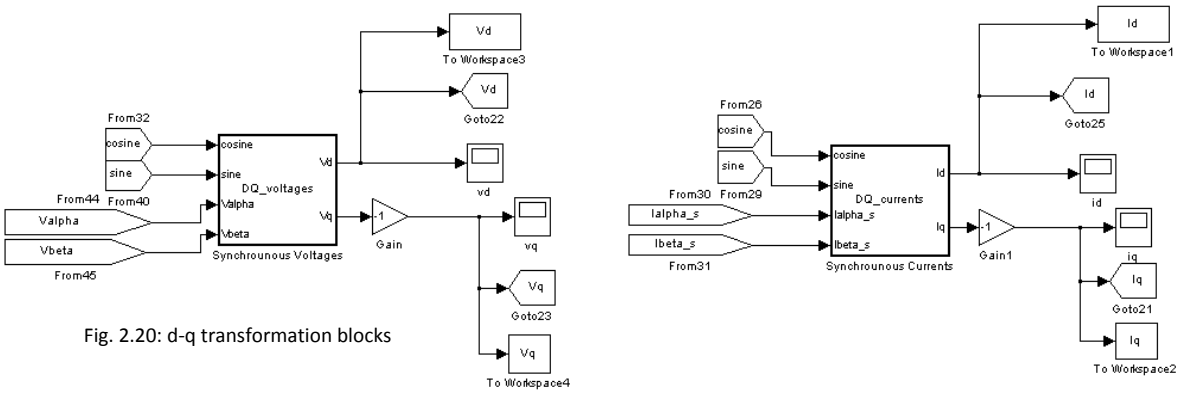

Fig. 2.20: d-q transformation blocks

Then, the *dq* components are filtered in order to get the mean value of their oscillations (above all in the switched inverter model) and so to obtain clearest signals.

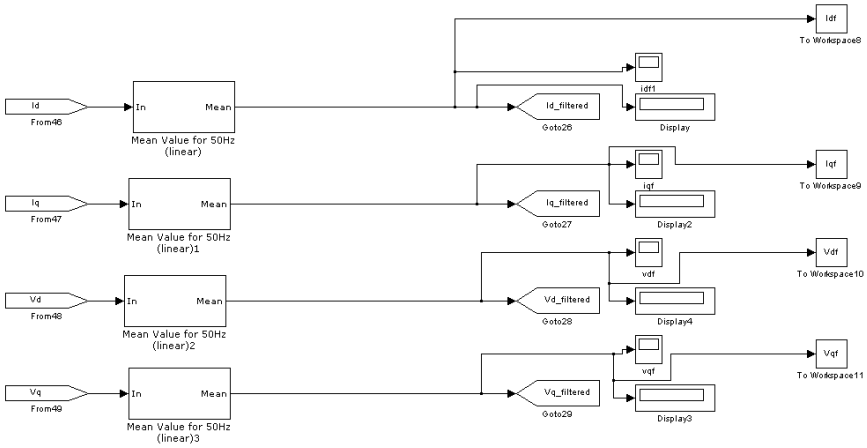

Fig. 2.21: the filtering stage of synchronous variables

2.9. The measurement and estimation blocks

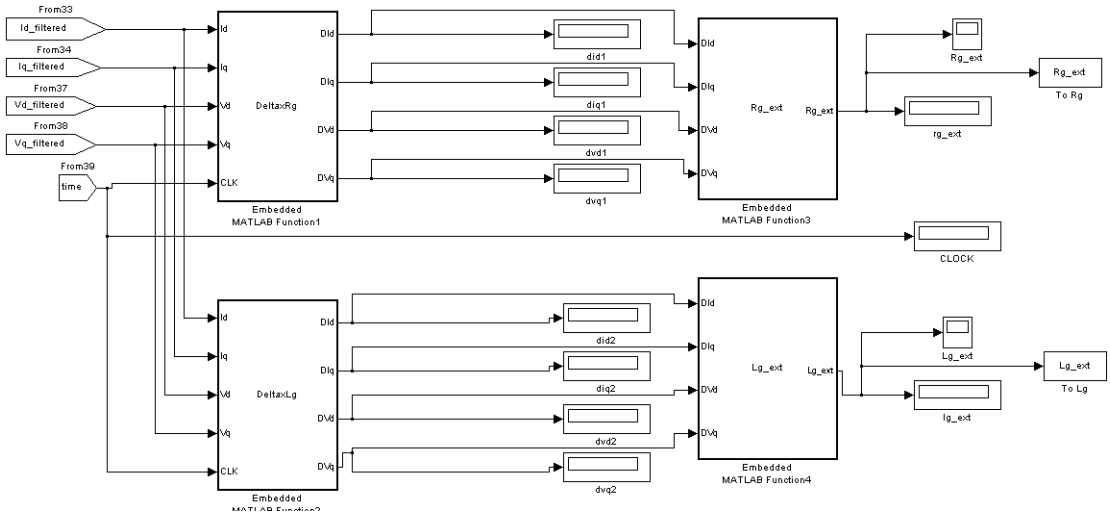

Fig. 2.22: the measurement and estimation stage

The filtered voltage and current components are sampled at precise instants experimentally chosen by considering the time required by the system to get the stability at the beginning of the simulation and after any power perturbation.

Before perturbing the active or the reactive power, the reference synchronous values are sampled both for grid voltage and grid current through the “DeltaxRg” and “DeltaxLg” blocks; once these values are acquired, the power perturbation takes place and, after a *fixed* time interval, new synchronous values are sampled. The “DeltaxRg” and “DeltaxLg” blocks’ outputs are the measure of the variation of these synchronous components after the power perturbation is terminated.

The estimated resistance and inductance values are given by the homonymous blocks: since the reactive power has been considered with an opposite sign, also the grid inductance formula should be changed of sign in order to get a positive value.

Both the four previous blocks are implemented as Embedded Matlab® Functions (see the Appendix)

Chapter 3

Simulation and results

3.1 Introduction

This chapter summarizes the plots and the final results obtained by simulations using both the average and the switched model of the inverter.

The simulations have been executed considering that the temperature and the solar irradiance are constant: i.e. the output characteristic of the solar panel doesn't change during the time.

Before starting the simulation, a Matlab script is executed in order to configure the parameters of the photovoltaic panel array. This script contains all the information about the size of the PV array, the physical parameters (someone related to the temperature) and the losses parameters used to implement the photovoltaic cell model.

The configuration script is shown below:

```
%%PV model parameters
clear all
clc

ns=750;
np=2;

q=1.6e-19;
k=1.38e-23;
Vgap=1.12;
eta=1.2;

T1=298;
Ish_T1=6.1/np;
Voc_T1=448.8/ns;

T2=300;
Ish_T2=6.1/np;
Voc_T2=442/ns;

irradiance_factor=0.0038;
Isat0=Ish_T1/(exp(q*Voc_T1/eta/k/T1) - 1);
cell_area=1e-2;
spectral_response=0.38;

Rs=1E-4;
Rp=1E4;
```

Once the script has been executed, the simulation can take place.

Before applying the PQ variation method, it is always necessary to wait a period of time in order to get the desired nominal point of work: this initialization time is not so important for understanding the results and some plots will not consider it focusing more on a precise time interval.

3.2 The simulation parameters

The following parameters are used in the simulations both in the switched and average model:

- Nominal reference active power P_{ref} equal to 2500W
- Nominal reference reactive power Q_{ref} equal to 0 Var
- Active power (step) variation ΔP equal to 10% of P_{ref}
- Reactive power (step) variation ΔQ equal to ΔP (also asymmetric perturbation is possible, since the power factor shouldn't be reduced too much in order to respect some standard regulations: in general, the minimum required power factor is equal to 0.9)

The obtained results have been divided by considering the inverter model.

The two Simulink models require different timing parameters (and execution time too) due to their different level of analysis; the grid resistance and inductance estimation has been executed once per simulation.

The Table 3.1 summarizes the used timing configuration:

Parameter	Average model	Switched model
Starting time for R_g estimation	**0.4 s**	**1 s**
Ending time for R_g estimation	**0.5 s**	**1.4 s**
Starting time for L_g estimation	**0.55 s**	**1.6 s**
Ending time for L_g estimation	**0.65 s**	**2 s**
Duration of a single estimation ΔT	**100 ms**	**400 ms**
Total estimation interval	**250 ms**	**1 s**

Table 3.1: The timing configuration

The estimation time and the time interval between the two components estimation of the switched model is longer than that of the average model since in the switched model it is necessary to wait a longer interval in order to damp the reactive power oscillations.

The timing of the proposed average model is the same that the original paper where an average model is used too. In the original paper no details are given about the time interval between the two grid impedance parameter estimations.

Both in the simulated models, the time interval between the two impedance components is an half of the duration of the single component estimation.

In any case, the estimation time is less than the maximum time required by many technical regulations in order to prevent the islanding phenomenon by disconnecting the photovoltaic system from the grid before this time is exceeded.

As mentioned in the original paper, the accuracy of the obtained results depend on the amount of the power perturbation and on the time interval ΔT of the single impedance component estimation. Since the time has been fixed, the effect of ΔP (ΔQ) and DC-link capacitor value will be analyzed.

The original paper doesn't consider this analysis: in fact, no details are given about the PV power source (i.e. the value of DC capacitor and the output characteristic of the PV array) and about the amount of power perturbation and their effects on the estimation.

During the development of this Thesis, the switched inverted model was implemented at first, and then, in order to reduce the duration of the simulation, the average inverter model has been considered.

Since the purpose of this Thesis is to highlight the effects of switching disturbances, as done in the original paper [5] too, the average inverter model at first and then the switched one will be analyzed.

3.3 The average inverter model's results

The average inverter model has been implemented in order to reduce the time required to simulate the complete system.

Since it is interesting to make a comparison between the behavior both of the implemented inverter models, almost the same graphs (but using a different time scale) will be illustrated.

3.3.1 The Grid voltage and current

The grid impedance estimation is obtained by changing the current phase and/or amplitude: the most visible variation of the grid current takes place during the grid resistance estimation process since the grid current amplitude is reduced in order to get a lower grid active power value.

The figure 3.1 shows the grid voltage and the grid current versus time during the grid resistance estimation process.

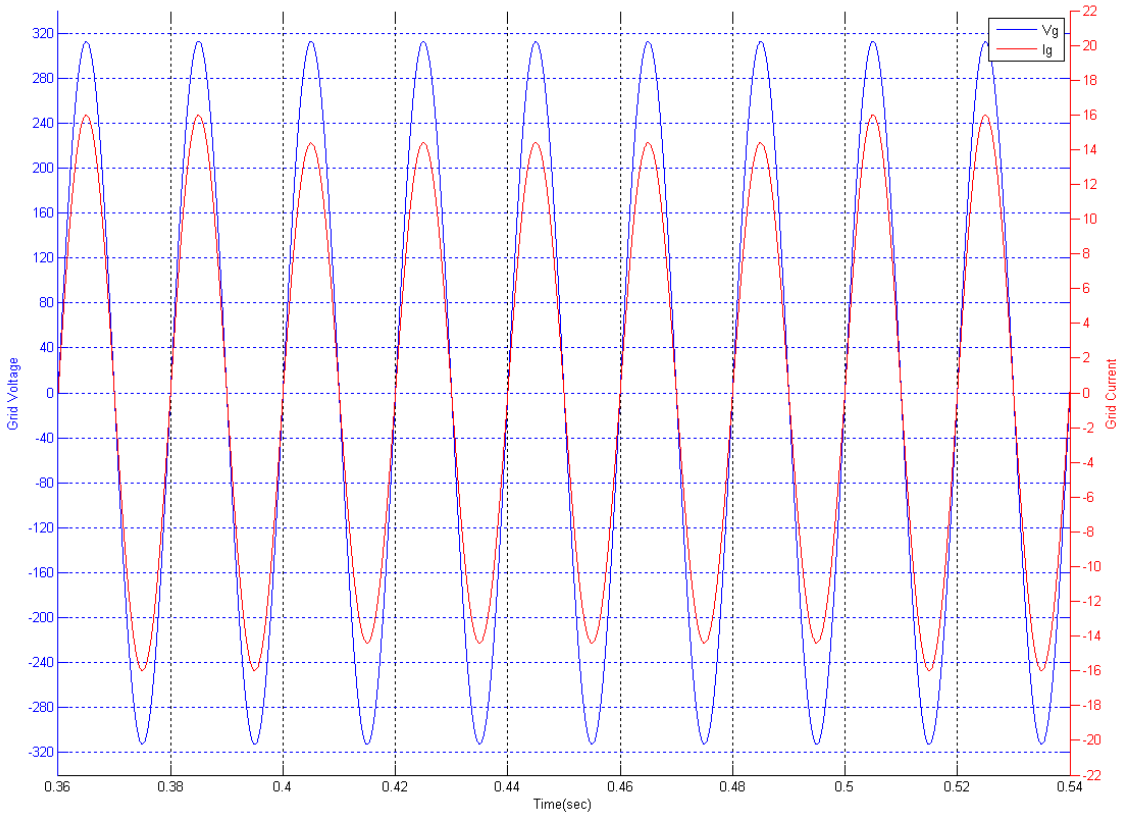

Fig. 3.1: The grid voltage and the grid current versus time

As it can be seen, here it is very clear that the two signals are well in phase and the amplitude current variation is easily measurable. In both the models, the only inductance L_f equal to 950 µH is used as output filter.

3.3.2 The R_g and L_g estimation

The grid resistance and inductance estimation process is illustrated the figures 3.2 and 3.3: here the use of Simulink Mean Block (used to calculate the mean value on the grid time period) is a little useless since the generated signals have been already average.

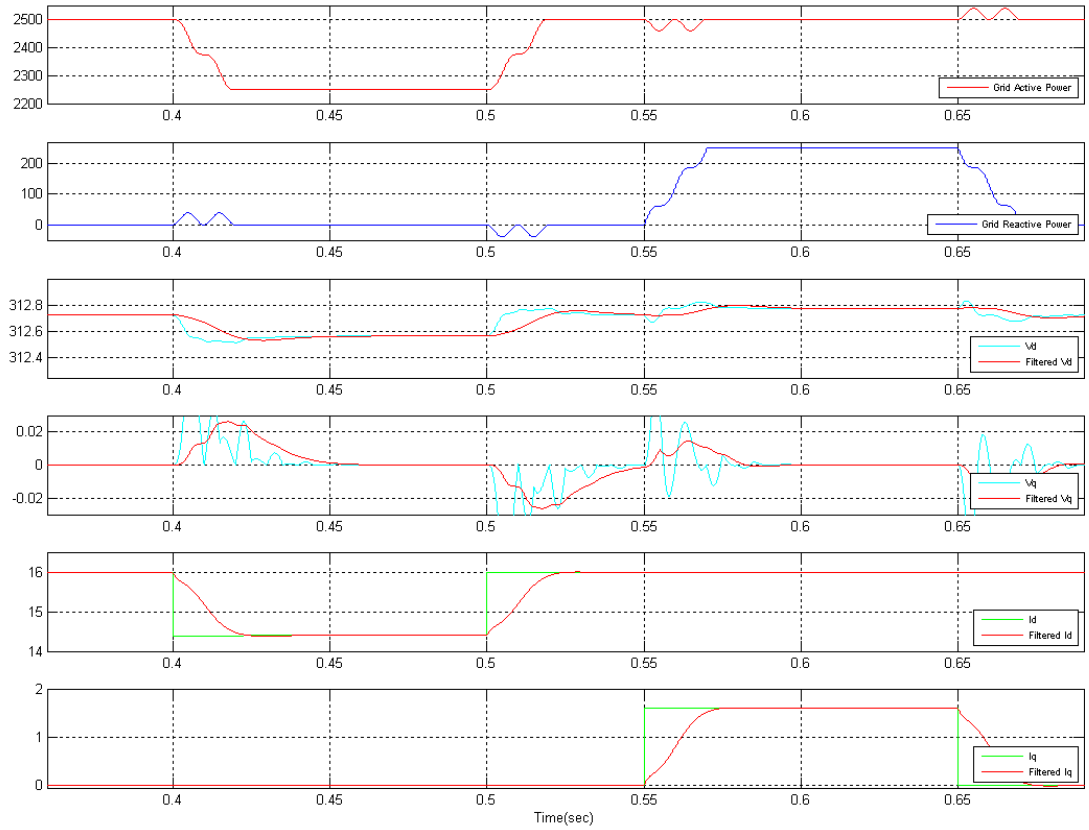

Fig. 3.2: The power perturbations and the consequent synchronous voltages and current variations

As the figure 3.2 shows, the instantaneous and filtered synchronous variables always reach, after a little transient during a power perturbation, the same value. It is really important to notice that, since also the grid voltage is average and noise-free, the instantaneous synchronous voltage is not affected by oscillations and that the instantaneous V_q component is always zero (neglecting the transients): by this way, the ΔV_q variation is always zero, as mentioned in the original paper, since the synchronous reference frame as been artificially build on grid voltage signal.

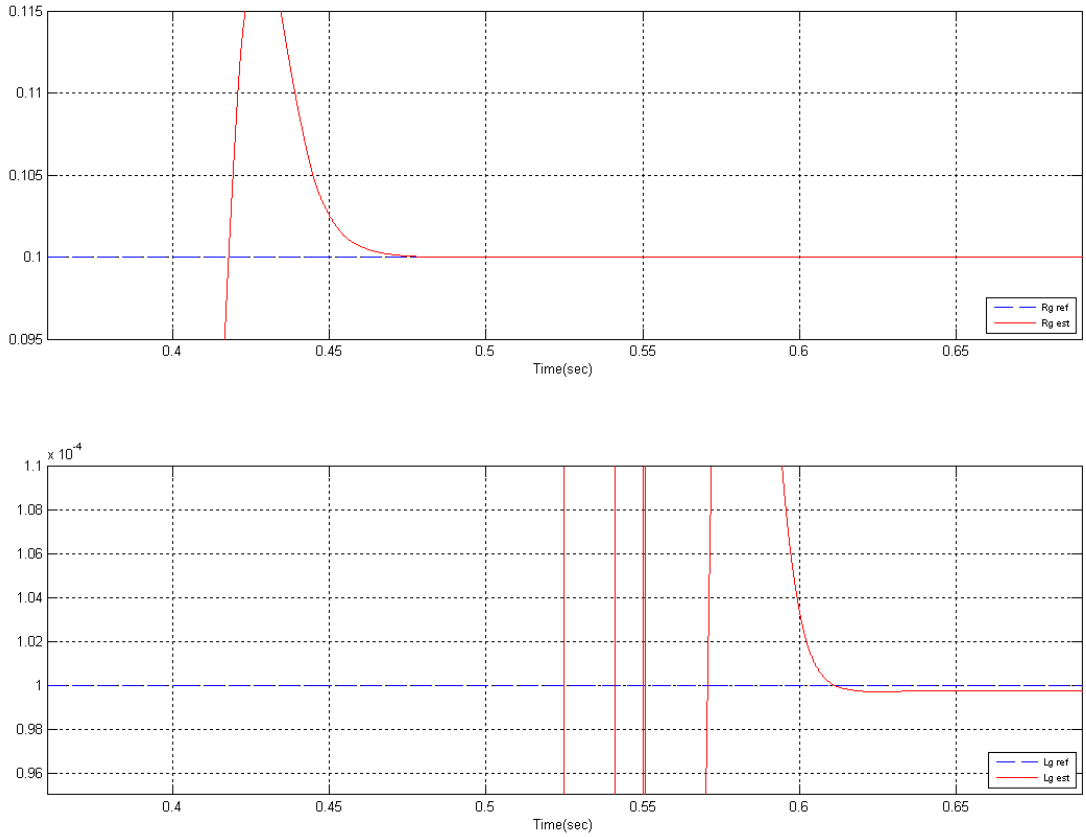

Fig. 3.3: The estimated Rg and Lg signals

In the figure 3.3, the grid resistance R_g signal reaches precisely the reference value at the end of its transient, while the estimated L_g signal is characterized by a constant error.

In both the models, the reference values are sampled at the same time both for R_g and L_g: by this way, the fact that the photovoltaic power hasn't reached its final value before grid inductance estimation takes place cannot affect the estimation performances.

3.3.3 The photovoltaic power source

The behavior of photovoltaic source respect to power perturbations is shown in the figures 3.4 and 3.5.

The reactive power tends to stabilize very quickly in the average model since the system is characterized by a general "smoothed" behavior with no need to oscillate continuously around the desired point of work as it could happen in a noisy scenario.

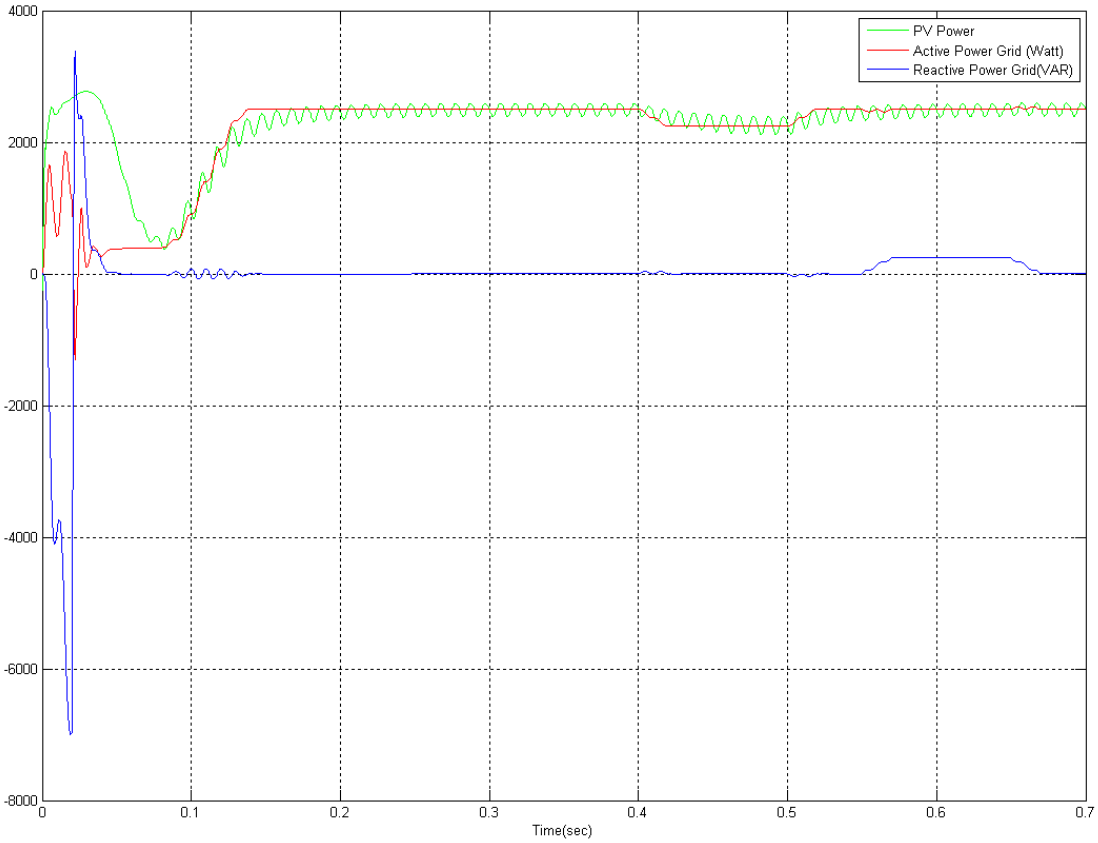

Fig. 3.4: The complete plot of PV, active and reactive powers

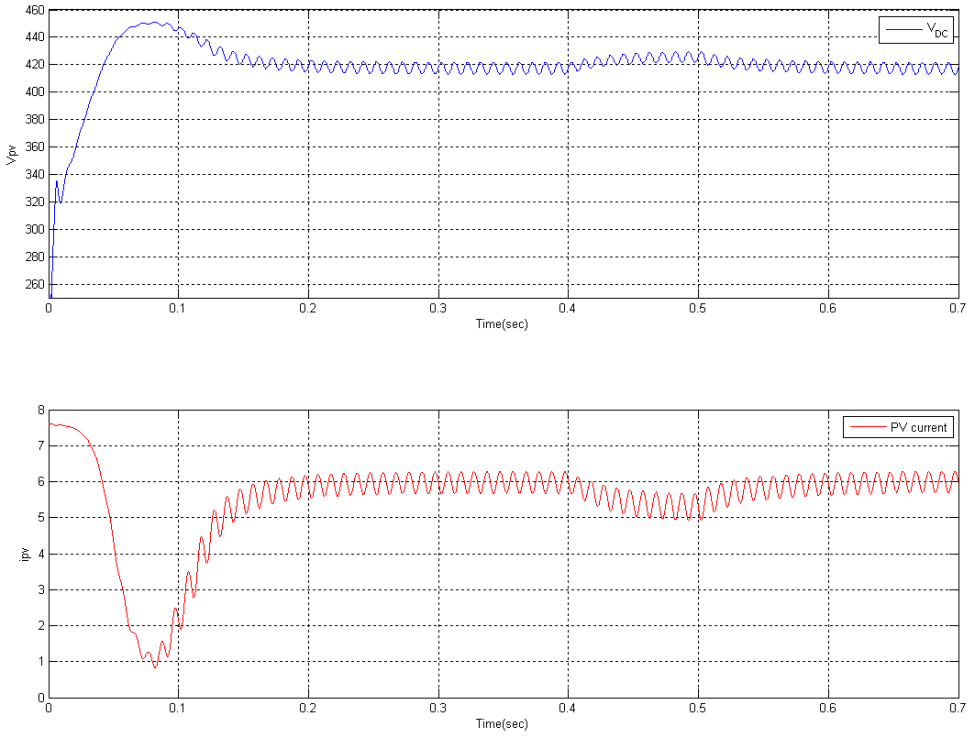

Fig. 3.5: The complete plot of PV, active and reactive powers

3.3.5 The effect of different amount of power perturbation on the estimation

The estimated resistance and inductance signal respect to the used power perturbation are illustrated in the figure 3.6.a and 3.6.b.

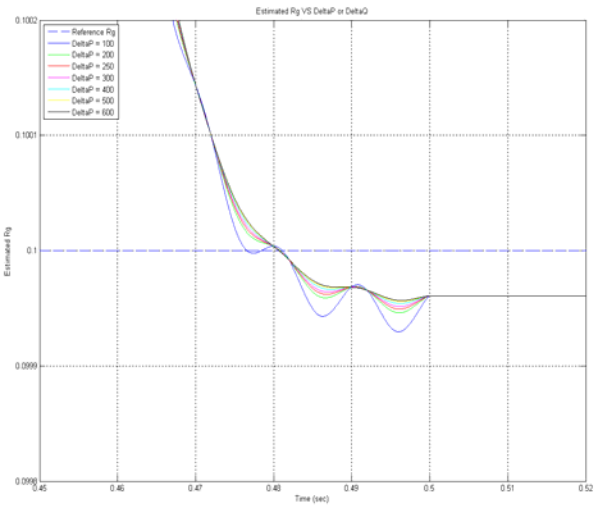

Fig. 3.6.a: The Rg signal respect to ΔP

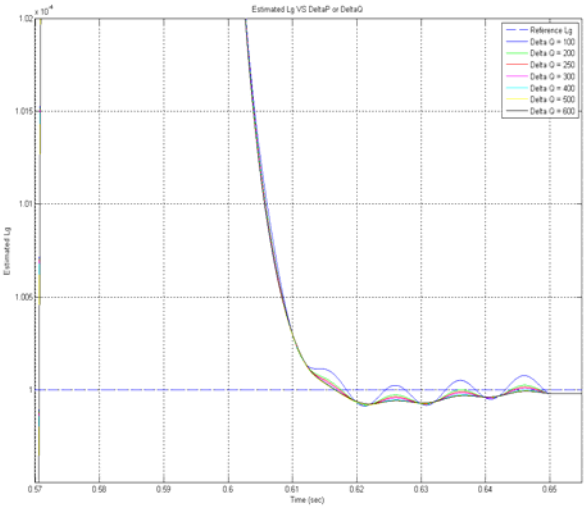

Fig. 3.6.b: The Lg signal respect to ΔQ

It has been checked that, independently from the active and reactive power perturbations, these signals always reach the same final value. The amount of power perturbation affects only the trend of the R_g and L_g signals.

3.4 The switched inverter model's results

3.4.1 The Grid voltage and current

The grid voltage and the grid current are shown in the figure 3.7, where it is highlighted the amplitude grid current reduction during the grid resistance estimation process.

It is easy to notice that the grid voltage and the grid current are well in phase during this operation. The grid current (and so the grid voltage too) is affected by harmonics even though the presence of the filter. Unlike the original paper where a LCL-filter is used, here, as mentioned, the used filter is just an inductance having a great value (L_f = 950µH) but this is not sufficient to reduce completely the noise.

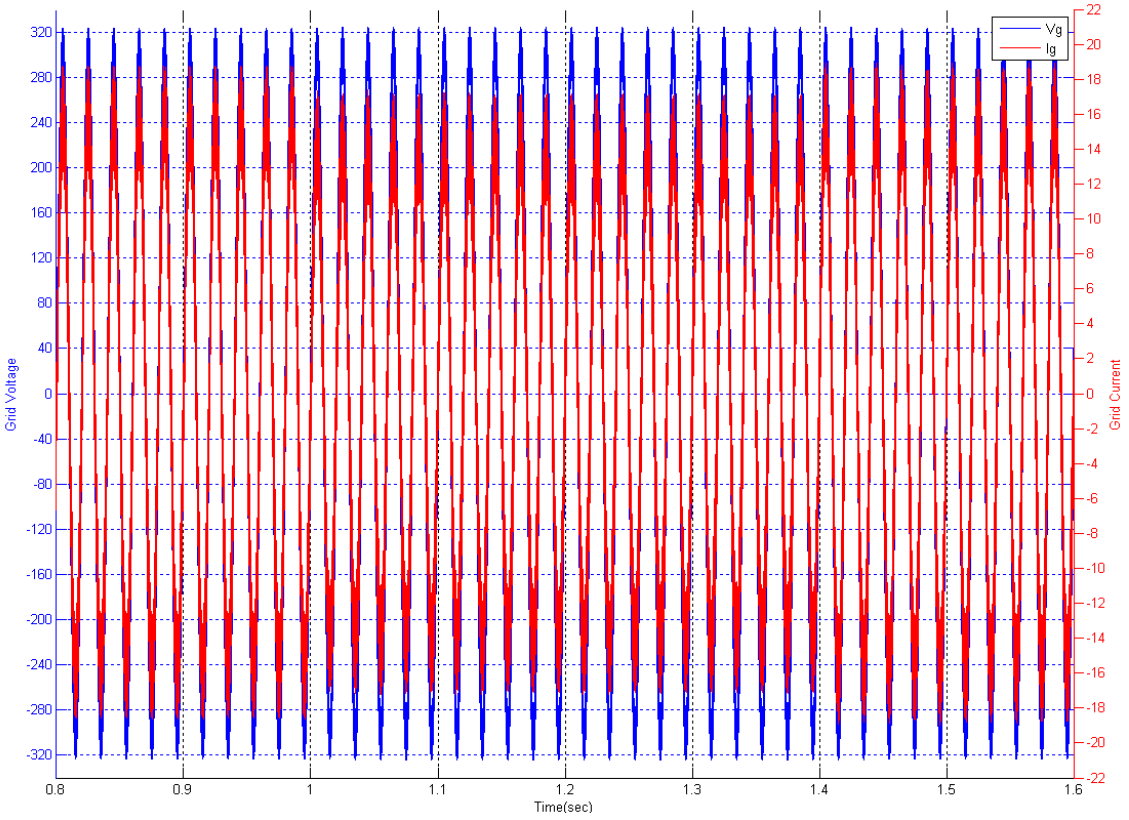

Fig. 3.7: Grid Voltage and grid current versus time during the resistance estimation process

3.4.2 The R_g and L_g estimation

In order to be consistent with the original paper, the line resistance and the line inductance values are equal to 0.1Ω and 0.1mH respectively and they are constant during all the simulation time.

The original paper estimates the grid impedance continuously during the time: since the aim of this Thesis is also evaluate the performances of the proposed method by focusing on the choice of parameters (such as the power perturbation) in presence of switching disturbances, only one estimation process is considered in order to better focus the obtained signals.

The full estimation process is illustrated in the figure 3.8: the synchronous currents and voltages variations due to power perturbations are illustrated. The figure 3.9 shows the estimated R_g and L_g signals.

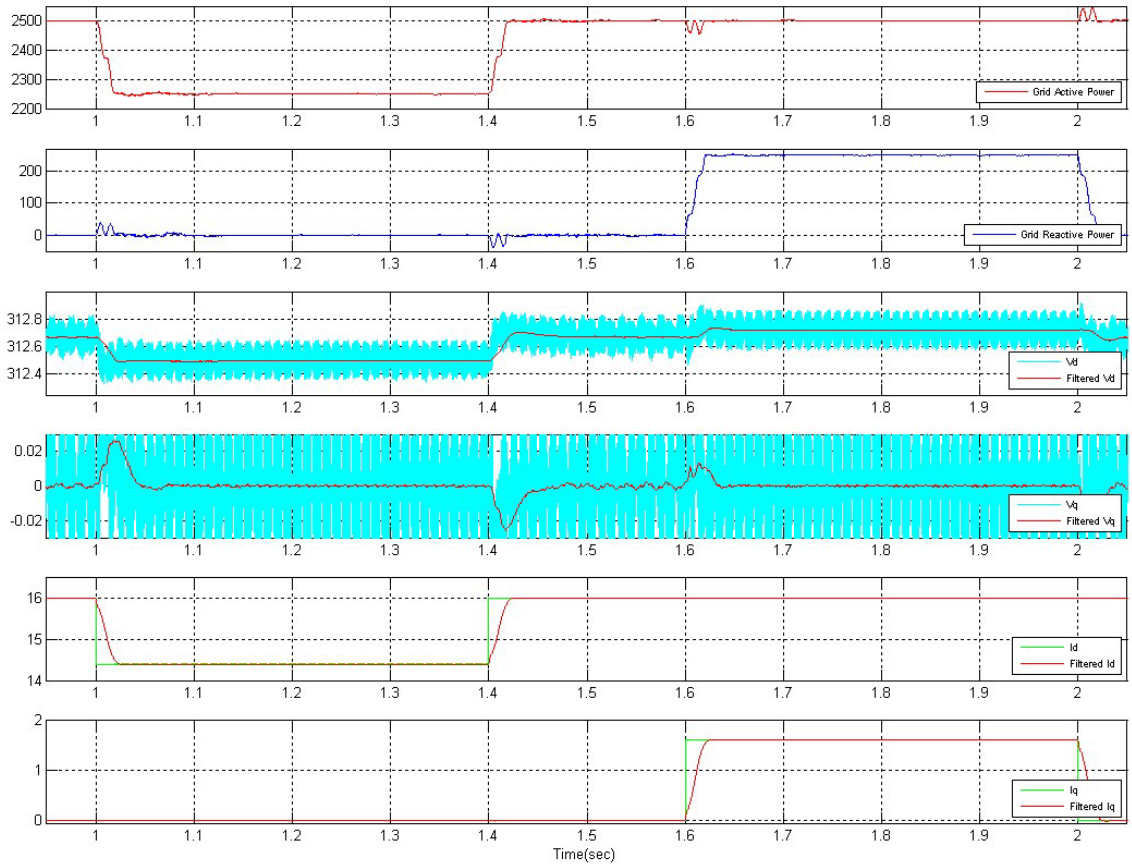

Fig. 3.8: The estimation process in the switched inverter mode

The most visible aspect in this simulation is a non-zero quadrature component both for line current (also it is not so visible due to the large vertical scale) and line voltage: it means that, due to introduction of these disturbs, the grid impedance components tend to oscillate around their mean value. Once the synchronous reference voltages and currents have been sampled (at 1 s), the grid resistance and inductance “signals” are continuously evaluated in order to analyze them over the time. Obviously, the evaluated signals are senseless out of measurement period.

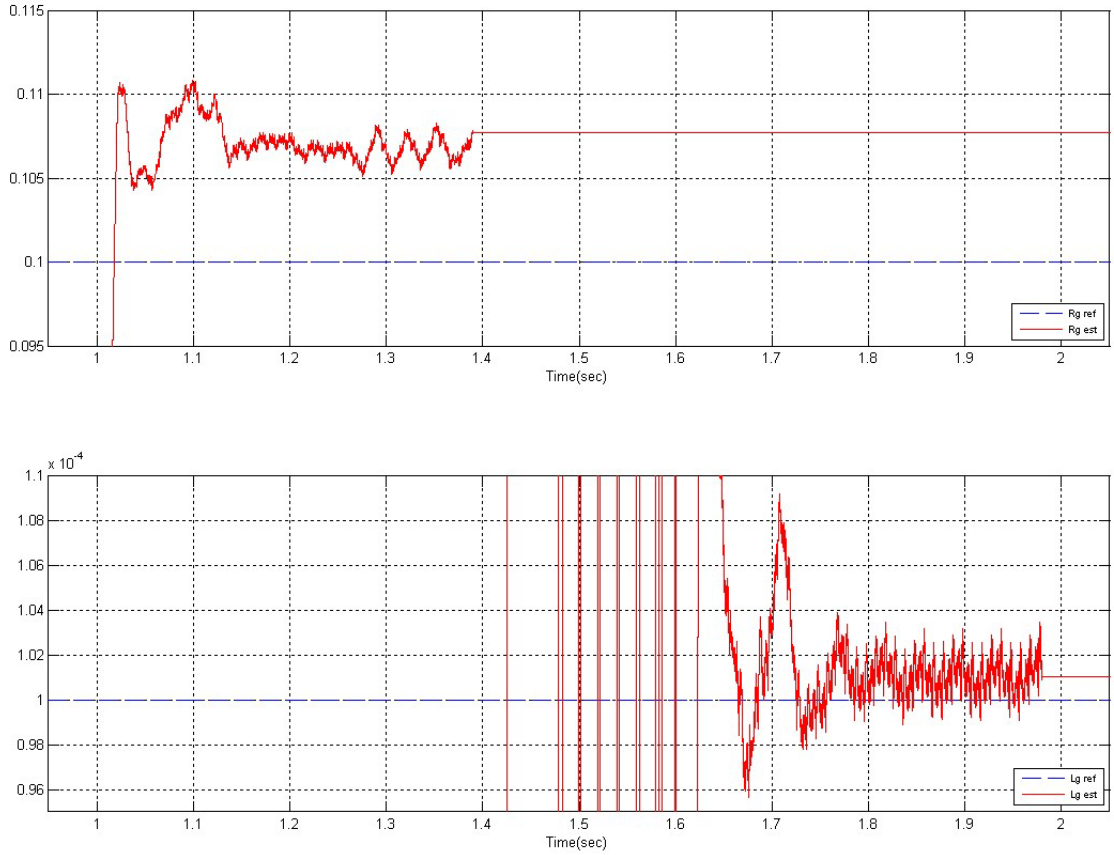

Fig. 3.9: The grid resistance Rg and the grid inductance Lg "signals" until the final estimated value is sampled.

As it can be seen in the figure 3.9, during any estimation period, the involved grid impedance component tends to stabilize itself as well as the system becomes more stable in its new point of work. Due to "oscillations" of synchronous variables, also the estimated R_g and L_g continue to show disturbances, even if a new steady state is obtained. Obviously, the instant of sampling of the estimated component is important since it decides for a value that can be nearest or not to the real component value.

The R_g and L_g instantaneous values depend on filtered synchronous currents and voltages: so, the used filter (in order to get the mean value of the instantaneous synchronous variables) totally influences the grid impedance estimation. As in the average model, also here a SimPower Mean Block is used in order to calculate the mean value on the grid time period: so the filtered synchronous values are simply *average* synchronous values without considering any filter dynamic. Using a properly filter, these oscillations could be also reduced but it is necessary to well define the filter dynamics (i.e. the filter time response or frequency response). Since, the aim is to evaluate how the method really works, not so much attention has been given to the filter's design.

In the figure 3.9, the reference values are sampled at the same instant for both the line impedance components, since by this way the new sampled values will be compared with the same references and, above all, the transient between the two power perturbations will not influence the measurement.

3.4.3 The analysis of the DC-link capacitor value

The transient period between the two estimations should permit the system to return to the previous point of work: it means all the system variables should get back to the previous values as soon as possible.

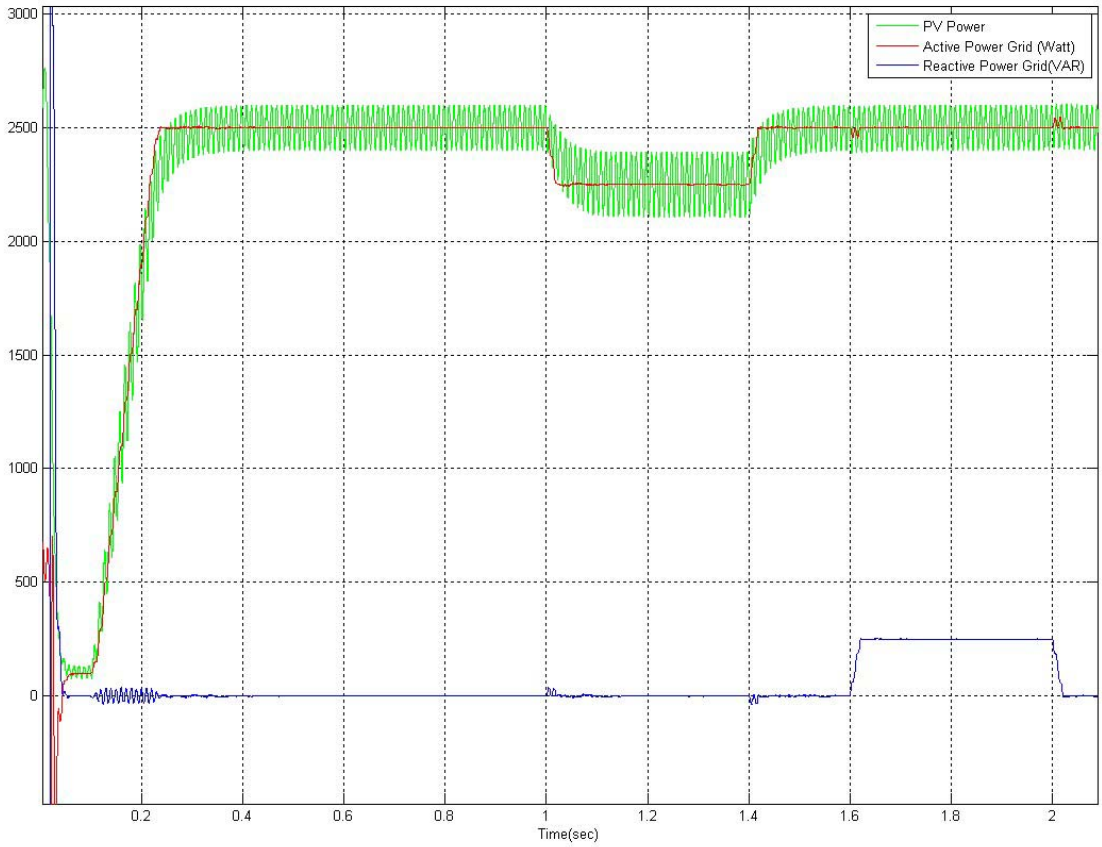

Fig. 3.10: Photovoltaic, Active and Reactive power during the simulation time

It is really important that, at the steady state and especially after a power perturbation, no reactive power oscillations occur in order to respect the required reference values and to restart a new estimation without being affected by noise.

If the last condition doesn't occur, the next estimation is affected by lower accuracy. These considerations could lead to think that it could be better to have a very fast system *in any case*.

For example, since the photovoltaic power changes more quickly by having a small DC-link capacitor value and it is necessary that also the input PV power is at steady state just before a new measurement, it could be easy to think that a very little DC-link capacitor value is required in order to reduce the interval between two estimations.

Indeed, in general, it is necessary to make a compromise between precision and time response. The figure 3.11 shows the photovoltaic, active and reactive powers respectively respect to the capacitor value.

The aim of capacitor analysis is understand which capacitor value is better in order to get the most accurate results both for line resistance and for line inductance too.

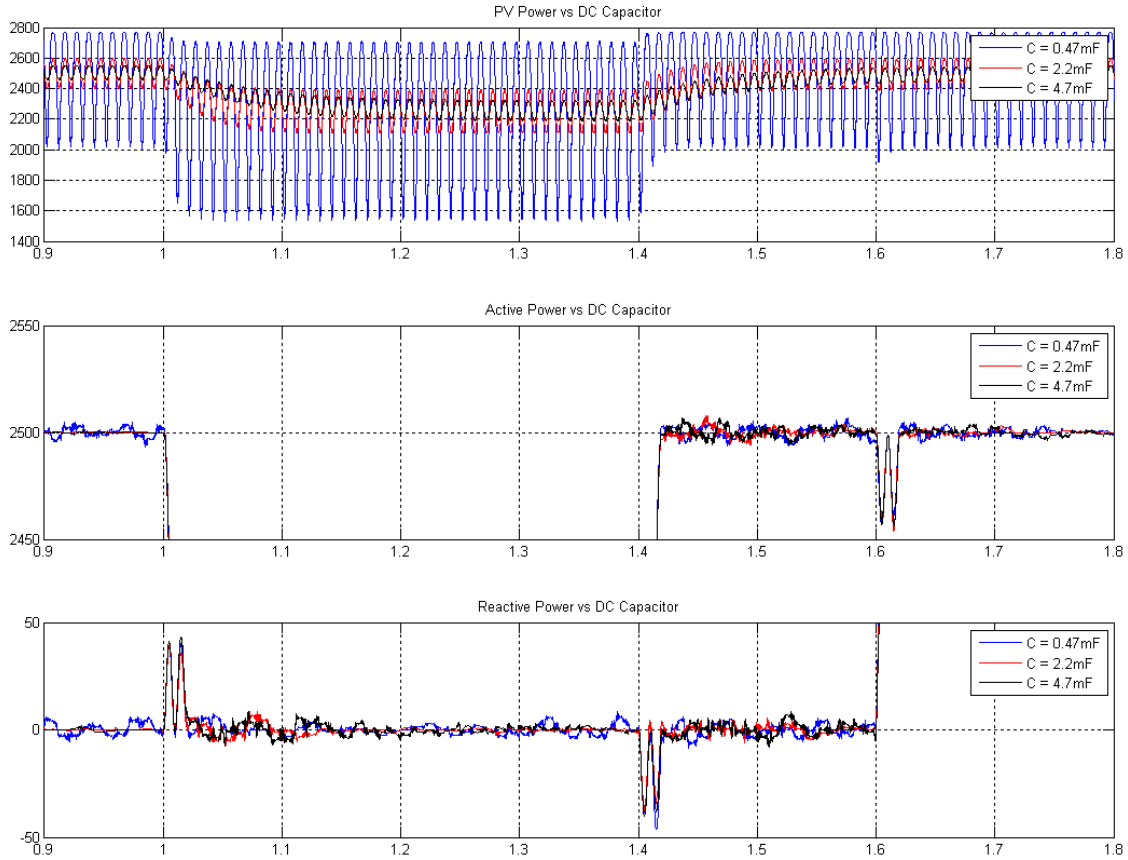

Fig. 3.11: The measured powers respect to the DC-link Capacitor value

By analyzing the figure 3.11, where three different values for the DC capacitor are used, the following possible cases can be considered in order to better understand the effects of these values on the estimation.

After an active power perturbation ends, even if the active and reactive powers have returned to their reference value, the photovoltaic power could not be at the steady state and this

means that the transient isn't really terminated (since a big non-zero reactive power value could be present): this means that in this case the used capacitor is too big; instead, by using a very small DC-link capacitor value, the PV power transient is very fast but a high reactive component is again present since more energy must be damped in a shortest time.

So, a good choice should lead to have an acceptable time response and, at the same time, a reduced reactive power oscillation: in this case the system variables (and especially the synchronous quadrature variables) tend to evolve in a smoothed way respect to the other cases and the point of work is easily acquired during an acceptable time interval.

The figure 3.11 shows that, before the resistance estimation, using the smallest capacitor a non-zero reactive power are present: i.e. the initialization time (of 1 second) is not sufficient to nullify it.

The better performance is obtained by using the 2.2mF capacitor and this coincides with the made choice. The figure 3.12 shows the obtained results respect to the DC-link capacitor:

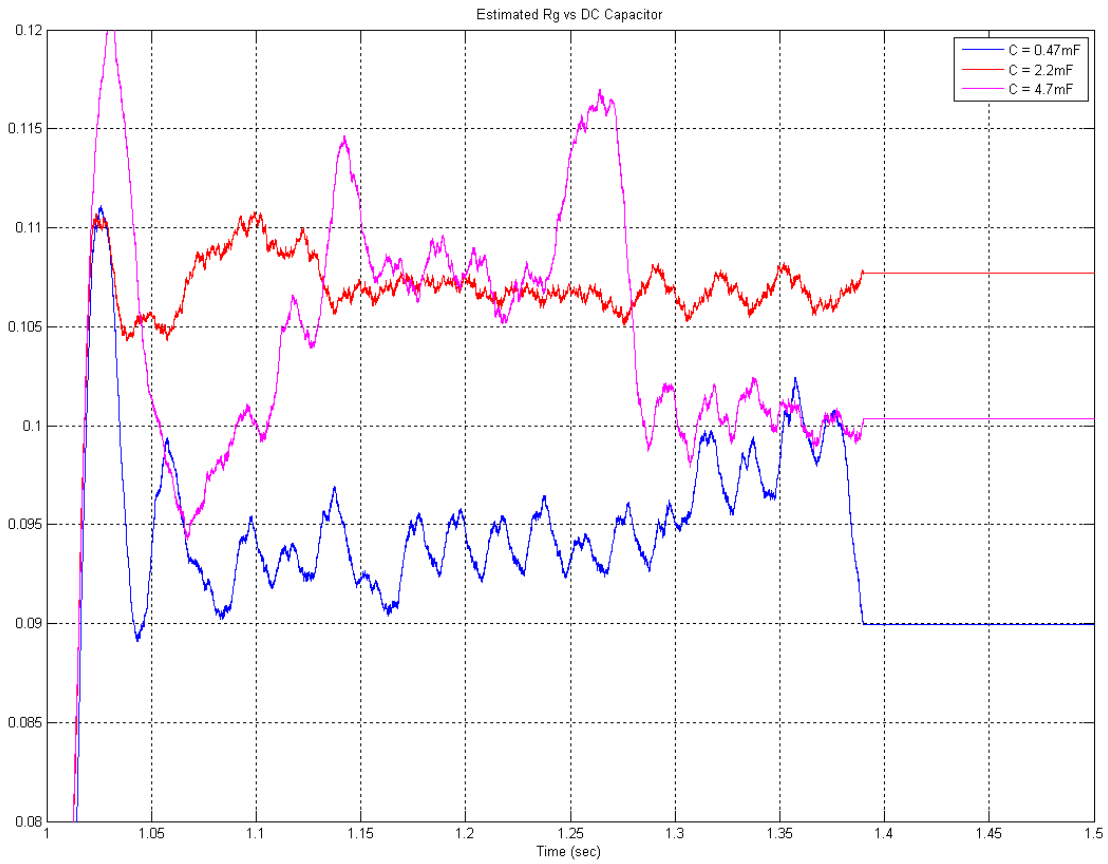

Fig. 3.12: The estimated line resistance respect to the DC-link Capacitor value

The estimated resistance value becomes stable very quickly using the 2.2mF capacitor; instead, the most precise value is obtained by using the greatest capacitor.

In the figure 3.13, the better inductance estimation is reached by using the 2.2mF capacitor again: it is clear that this estimation is more influenced by capacitor value since it follows the resistance estimation after a *finite* time interval. The biggest capacitor value affects a lot the precision of the resulted inductance estimation due to always present transients.

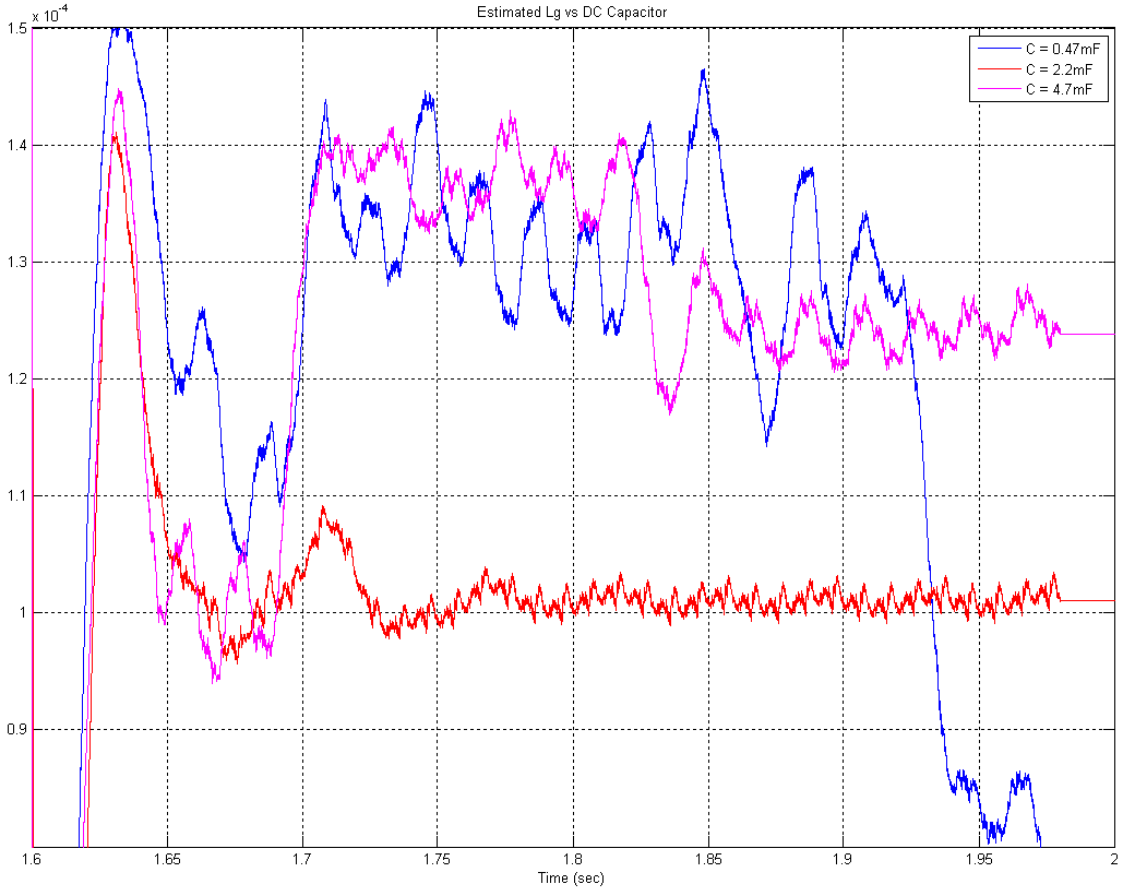

Fig. 3.13: The estimated line inductance respect to the DC-link Capacitor

In effect, the figure 3.13 is also a measure of effects of unfinished transients on the estimated inductance value.

3.4.4 The photovoltaic power source

The capacitor value is so related to the time required to dispose of the stored energy capacitor itself after any active power perturbation.

An active power reduction lead to a voltage capacitor increase and an output photovoltaic current decrease as the PV output characteristics suggest (see the figures 2.5 and 2.6). The figure 3.14 shows these effects: it could be interesting to notice that these variables don't change during the reactive power perturbations.

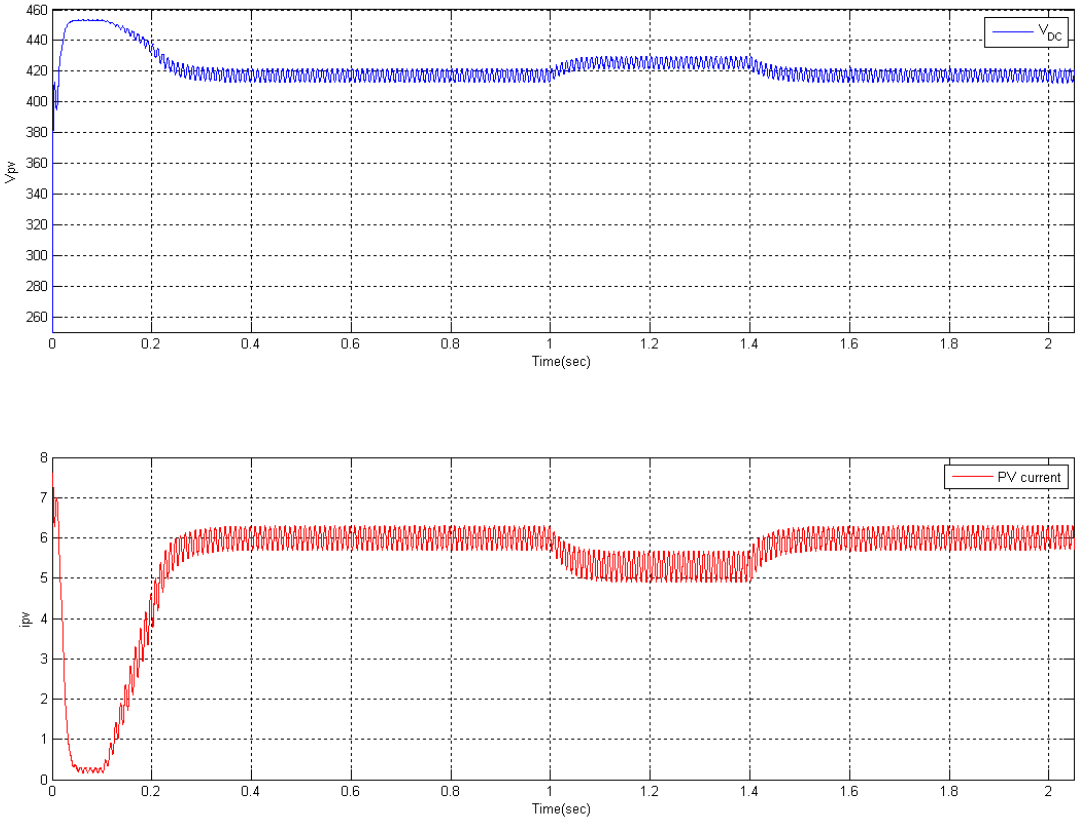

Fig. 3.14: The DC-link voltage capacitor and photovoltaic current with 2.2mF capacitor

3.4.5 The effects of different amounts of power perturbations

In a similar way, if a capacitor value has been fixed, it could be interesting to analyze how different perturbation values affect the grid impedance estimation.

In the original paper an active and reactive power perturbation equal to the 6.6% of the reference active power (1.5 kW) has been used.

The choice of the active (and reactive) power perturbation value should be made basing on two main qualitative considerations:

- Since a switched inverter model with its disturbances is here considered, using a too small power perturbation, both the resistance and inductance could be affected by a not negligible error. So, it means that, in the switched model, the two point of work cannot be too near.
- On the other hand, if the perturbation is too big, again the amount of energy to be disposed is high respect to the fixed time interval between the two estimations.

In general, by using the switched inverter model, the accuracy of the estimation increases as the power perturbation and the delay between the estimations increase. Since the time should

be as short as possible, it is necessary to understand how much the power can be changed without reducing the performances.

The figure 3.15 and 3.16 show the estimated resistance and inductance “signals” respect to different power perturbation values.

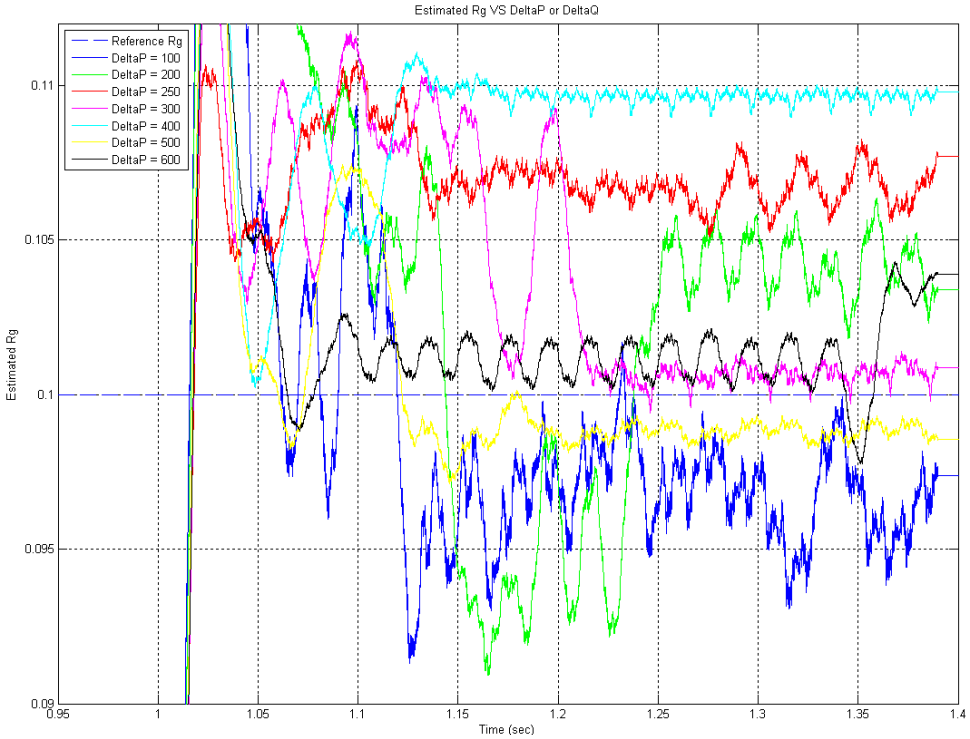

Fig. 3.15: The estimated Rg signal respect to different active power perturbations

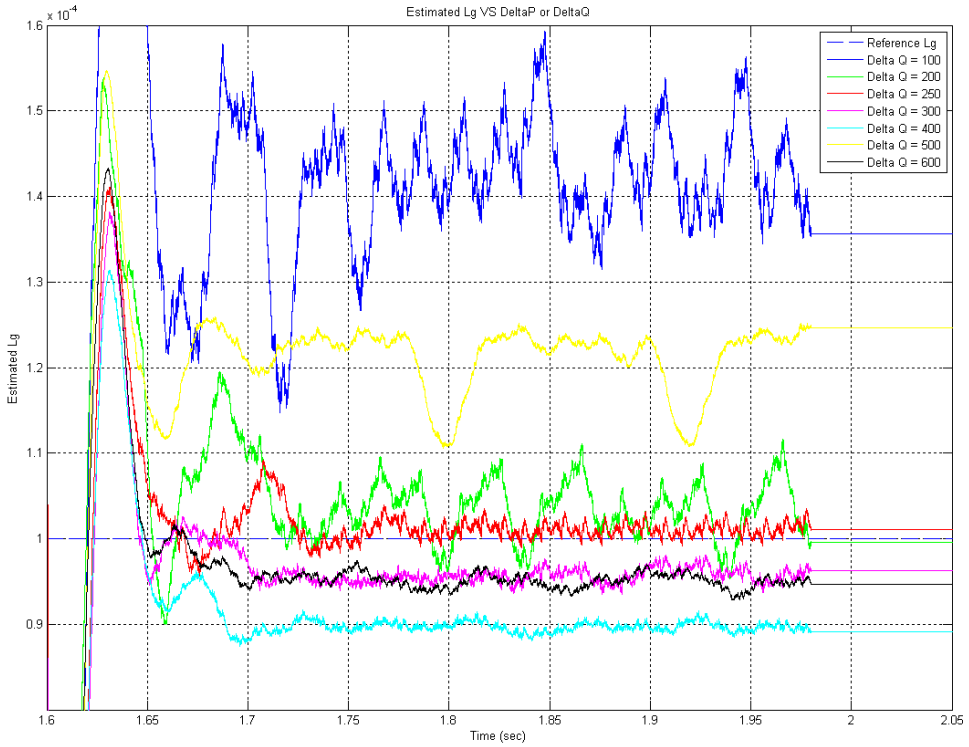

Fig. 3.16: The estimated Lg signal respect to different active (reactive) power perturbations

Both the resistance and the inductance estimation have a good accuracy, but from the figures 3.15 and 3.16 it is clear that different time trends are obtained by using different amounts of power perturbation. If the lower perturbation is considered, both the signals are more affected by noise; instead, increasing the amount of perturbation, the role played by reactive disturbances on the general trend is least significant, and, independently from the sampled final value, the reached stability is better as the perturbation increases. The mean value of this trend and the final sampled value of both the impedance components are instead influenced by the reactive non-zero components due to some transients still in progress. In many case, a very little variation of reactive components lead to great instability of these signals or simply it is able (if the variation is quite constant) to distance the curves from the reference values.

The figure 3.17 shows that, also using a reactive power perturbation of 600 Var, the power factor is always over the minimum required value of 0.9.

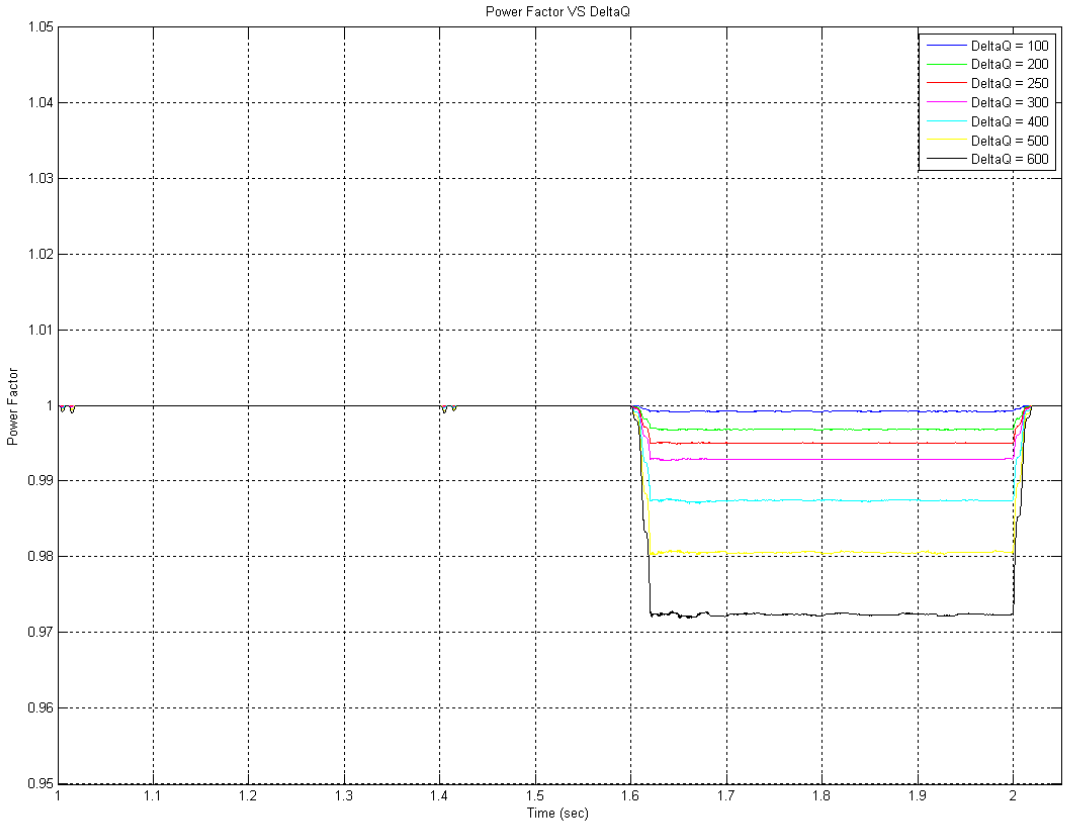

Fig. 3.17: The power factor VS different reactive power perturbations

3.5 The final results

The obtained results have been summarized in the Table 3.2.

ΔP or ΔQ	Average model		Switched model	
	R_g [Ω]	L_g [H]	R_g [Ω]	L_g [H]
100	0.09996	0.998E-5	0.09739	0.0001356
200	0.09996	0.998E-5	0.1034	9.958E-5
250	0.09996	0.998E-5	0.1077	0.000101
300	0.09996	0.998E-5	0.1009	9.63E-5
400	0.09996	0.998E-5	0.1098	8.913E-5
500	0.09996	0.998E-5	0.09855	0.0001247
600	0.09996	0.998E-5	0.1039	9.471E-5

As mentioned, using the average model, the final result hasn't been affected by noise and always it has given the same value.

The final results, by using the proposed parameters and models, have been highlighted.

Chapter 4

Other issues about the Standard PQ Variation Method and final remarks

4.1 Limitations of the Standard Method

In the previous chapters, the proposed PQ variation method and its performances have been evaluated: in particular, the chosen parameters, the role played by the switching harmonics of the *ideal* inverter and by the reactive power disturbances have been discussed.

The proposed method has been applied under three important assumptions:

1. The line impedance is linear: this is the main desired condition for all controllers. First of all, the grid impedance isn't simply a first order transfer function but it should be modeled by a transfer function whose order depends on the micro-grid dimensions and complexity. The hypothesis of linearity leads to apply easily the principle of superposition.

2. The grid impedance components (R_g and L_g) are constant

3. The grid-side sinusoidal voltage V_s doesn't change over the time its amplitude, phase or frequency. A frequency change, for example, affects the operation of the SOGI since it is centered on the grid frequency while an amplitude and/or phase change affects directly the estimation (see the eq. 1.37).

In the figure 4.1, an active and reactive power perturbation is shown. The active power perturbation starts at 0.4s and it has a duration of 60ms; the reactive power perturbation begins immediately after the active one and it has the same duration of the previous interval. In this figure, the reference synchronous voltage and current values are sampled at 0.4s and, in order to calculate R_g and L_g, the new synchronous voltage and current values are sampled at the end of any interval.

If one of these parameters above (R_g L_g and V_s) changes between two different estimations, the presented PQ Variation method works properly, especially when the reference values of the synchronous voltages and currents are sampled just before the single estimation component starts. In fact, in this case, all the estimations are independent.

In any case, this is not true if some change happens just before sampling the reference or the new synchronous voltage and current values, since the generated reactive power transient affects the estimation by perturbing these values respect their real values.

In the figure 4.1, the four possible subintervals during which the micro-grid could change some of its features are indicated:

1. Before any power perturbation (the first brown arrow).
2. During the transition between the two steady states (the first black arrow)
3. During the interval the system is at the new steady state (the second black arrow)
4. At the end of a power perturbation (the last brown arrow)

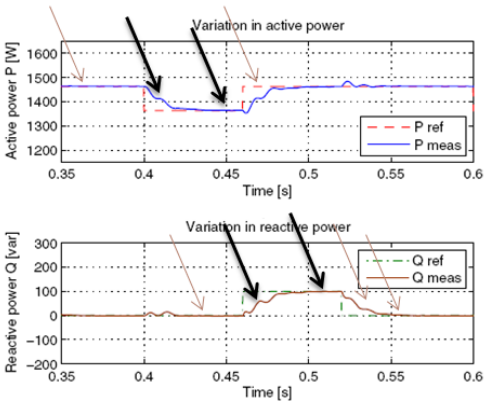

Fig. 4.1: The micro-grid could change its features in four possible moments: the black arrows show the most dangerous for the performances of the PQ Variation method.

It has been observed that any change in the grid parameters (R_g, L_g and V_s) generates a reactive power transient. No reactive power transients due to these *external* changes are shown in the figure 4.1, but only the power perturbations used to apply the PQ variation method.

By monitoring the reactive power, it could be possible to detect some external grid change: this is possible if the reactive power is simply constant.

The black arrows, in the figure 4.1, indicate the sub-intervals during which is more difficult to detect a reactive power transient due to some grid parameter change since it is not possible to distinguish between the transient due to the power perturbation and the transient due to the external grid variation.

By using the PQ variation method proposed in the previous chapters, if a grid parameter change happens during the sub-intervals indicated by black arrows in the figure 4.1, the estimated values are sure wrong and there isn't a way to correct them.

In fact, after a power perturbation, considering that the new values are sampled at the end of estimation period, if some parameter changes during the initial transient or when the new stability condition has been reached, new reference values are needed in order to make a correct estimation.

Probably, a resistance or inductance variation is not so dangerous like a grid-side voltage variation. If R_g or L_g changes during the initial transient the estimation will be probably good since it depends on the variations of currents and voltages only and not on their absolute values; so, the estimation will be probably affected by an error that is not negligible only when these changes happen in proximity of the end of any estimation interval.

Of course, a grid-side voltage variation has a bad effect on the results if it happens during the estimation period since, by definition, the standard PQ variation method cannot be applied in this case.

4.2 A proposal of a Modified PQ Variation Method

If the system has reached its steady state, the reactive power (as requested during the normal operation) should be zero or equal to its constant reference value. If a grid parameter changes, the effect on the *average* reactive power is the presence of a transient.

In the switched version of the system, the instantaneous reactive power is generally different from the zero value: in this case, it should be more useful to analyze the average value of the reactive power. In the average system this is naturally done! So, in a switched model the instantaneous reactive power should be average on a certain number N of samples.

The presence of a transient can be also justified considering that, if some branch or power source in the micro-grid is connected or disconnected, all these three parameters (R_g L_g and V_s) could change together and this superimposed variation is sensed differently at any node of the micro-grid as a transient.

Basing on these concepts, a modified PQ variation method can be proposed in order to overcome the limitations of the standard one.

4.2.1 The basic principle of the new proposal

The standard PQ Variation Method estimates the grid inductance components basing on the sampled values at fixed instants of time and using fixed durations of the estimation interval:

both these parameters don't take into account the operating status of the system (if a steady state has been reached or not) but their choice has been delegated to the designer. Generally, the designer could make his choice based on experimental results and his observations.

Since the reference values both for active and reactive powers are known, the first aim of a new proposal is surely to ensure that the estimation starts and ends when the required steady states are obtained before and after a power perturbation. So, the first aim of a modified PQ Variation Method should be its adaptability the connected grid obtained by evaluating automatically if the steady state has been reached or less by the system.

As mentioned, the new proposal is based on the monitoring of the average reactive power in order to sense some spike or transient due to some micro-grid topology variations.

Since the PQ Variation method is based both on active and reactive power perturbation and since the perturbation of a specific power affects the other one, it could be interesting to explore how the power can be perturbed without generating high transients in the system. For example, the figure 3.13 in the previous chapter shows that a step active power perturbation generates a not negligible reactive power transient.

Indeed, since some micro-grid parameters variation could happen at any time, it is really important to highlight always this disturb respect to the average reactive power value: i.e. the active power should be perturbed in way that the reactive power isn't affected so much by very high transients. So, instead of using a step power variation, a *low slope* ramp power variation could be applied in order to perturb in a *controlled way* the reactive power.

The terms "low slope" and "controlled way" are qualitative concepts: i.e. the duration of the power perturbation cannot be too long because it is upper bounded by regulations and by practical usability of the method itself and lower bounded by admitted maximum reactive power variation during any estimation. From a very simple point of view, if the average reactive power value is, at any instant, greater than this upper limit a spike is detected and the estimation process (if it's in progress) should be stopped since the estimated values are wrong; after the system has reached again its reference steady state a new estimation process can be repeated.

4.2.2 A possible Simulink-based approach to the modified algorithm

An adaptive algorithm can be implemented using Matlab®/Simulink without changing the scheme of the standard PQ Variation Method: the only difference is that the reactive power is monitored and that, instead of using an independent step power perturbation signal, the perturbation is adapted to the instantaneous value assumed by the average reactive power in order to maintain it to an acceptable very low level without increasing a lot the duration of the estimation process.

A possible way to proceed is to define two different thresholds: the first is related to the *controlled* perturbation of both the powers, the other one (bigger than the first) is related to the transient detection; nothing happens if the average reactive power value is between these two thresholds.

The basic principle is to increase/decrease the involved power perturbation by a little percentage of the total variation when the average reactive power is less or equal the lower threshold and to stop the estimation process when the average reactive power is over the upper threshold. By this way, the average reactive power is maintained to a value between these two thresholds.

The threshold values affect both the timing and the performance of the new proposed method. These values can be estimated or by experimental results (in a training phase) or through some special algorithm in order to adapt the method to any micro-grid.

In the next, a Simulink-based approach to a new proposal is presented.

In order to run alternately the two grid impedance components estimation and to memorize the actual status of the process some flag is introduced: the variable *flag* memorize which is the next estimation to do, while the variables *state_Rg* and *state_Lg* memorize which estimate is in progress. Another adaptive property is that if a spike is detected not only the estimation process is stopped but the lower threshold becomes an half of the previous value in order to be sure that the detected event isn't due to a bad choice of the lower threshold: in any case a new estimation is repeated as soon as the system reaches the steady state again.

4.2.3 A Simulink-based approach flowchart to the new proposal

The figure 4.2 shows a possible flowchart in order to implement the modified PQ Variation Method using Simulink.

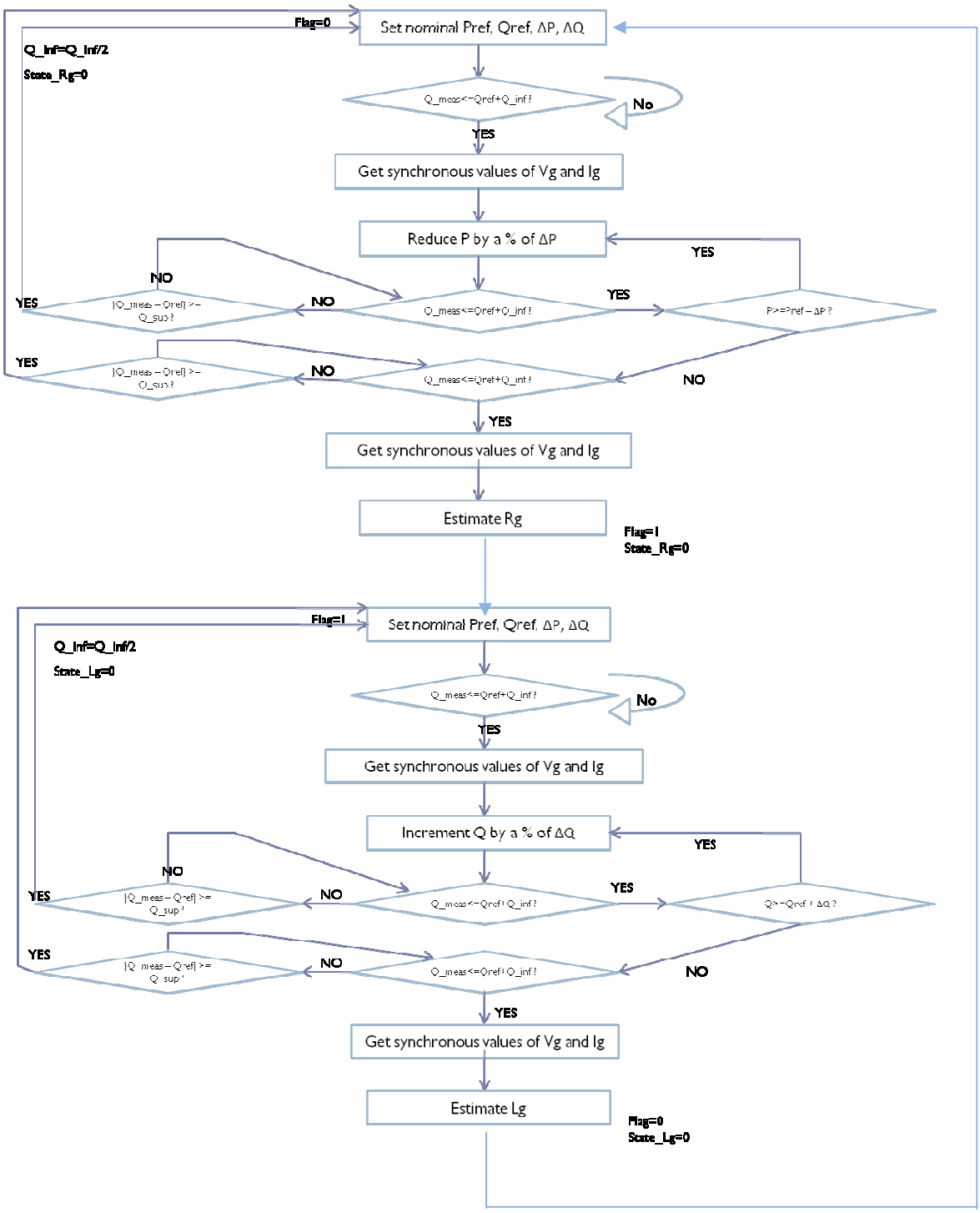

Fig. 4.2: The new proposal flowchart in a Simulink-based approach

In the fig. 4.2 the variable *Q_meas* is the monitored average (over N samples) reactive power.

The flowchart shows that the reactive power is monitored and controlled both during the power perturbation, after this perturbation has ended and until the new synchronous values are sampled (when it is sure the new steady state has been acquired).

4.2.4 Some initial result

A first attempt of a modified PQ Variation Method has been implemented in Simulink using the flowchart shown in the figure 4.2.

In order to evaluate the performance of this new proposal respect to the standard PQ Variation Method, the scenario summarized in the table 4.1, where an external grid change occurs at 2.5s, has been considered.

	Before 2.5s	After 2.5s
Rg	0.0466 Ω	0.0467 Ω
Lg	99.765 µH	99.897 µH
Amplitude of Vs	310.4467	310.5711
Phase of Vs	-3.7652E-4	-0.00012

Table 4.1: The values of grid parameters used in the simulation. The variation of these parameters at 2.5 is very little.

By comparing the results obtained by applying the standard PQ method and the new proposal, a first analysis about the performance of the modified method will be made.

The figures 4.3, 4.4 and 4.5 show the obtained results applying the standard PQ method, while in the figures 4.6, 4.7 and 4.8 the first obtained results using the new proposal are illustrated.

Applying the Standard PQ Variation Method, as it can be observed in the figures 4.3 and 4.4, by neglecting the grid change at 2.5s, a very high estimation error occurs and the next resistance estimation should be expected in order to get a correct resistance value. The line inductance estimation isn't affected by the grid change.

In the figure 4.5, the large transient due to the external grid parameters has been shown: it is interesting to highlight that a very (superimposed) little variation of all parameters lead to a very high reactive power transient.

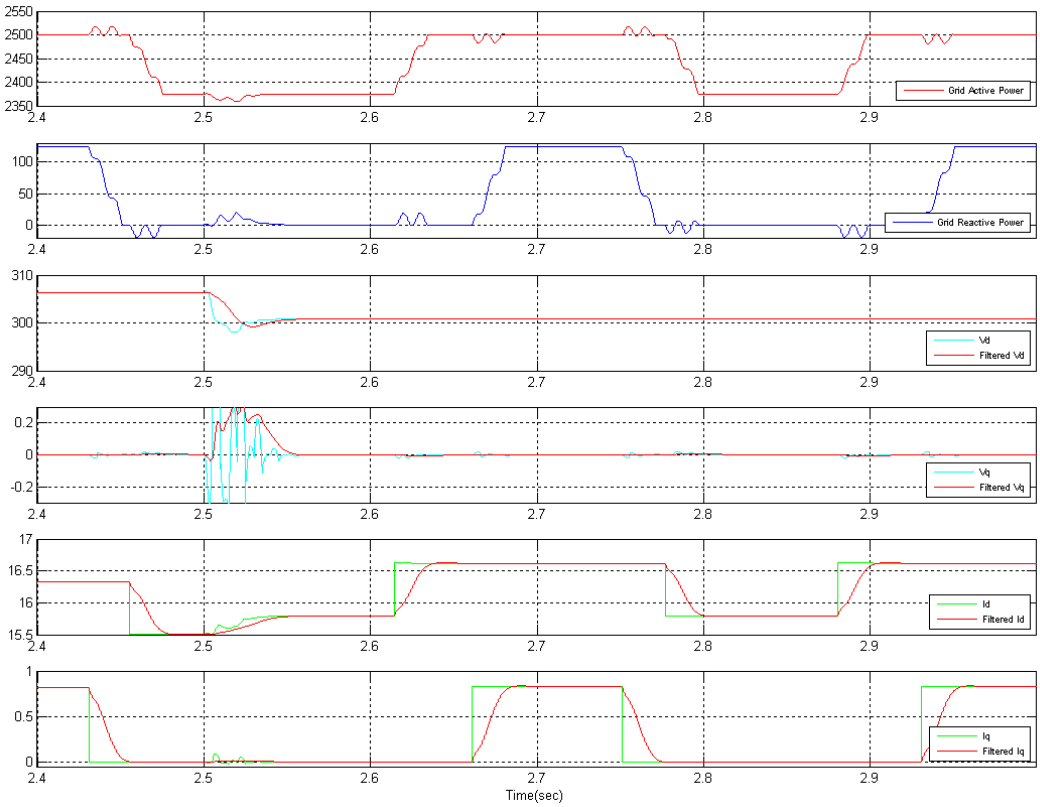

Fig. 4.3: The synchronous voltage and current signals obtained applying the Standard PQ Variation Method

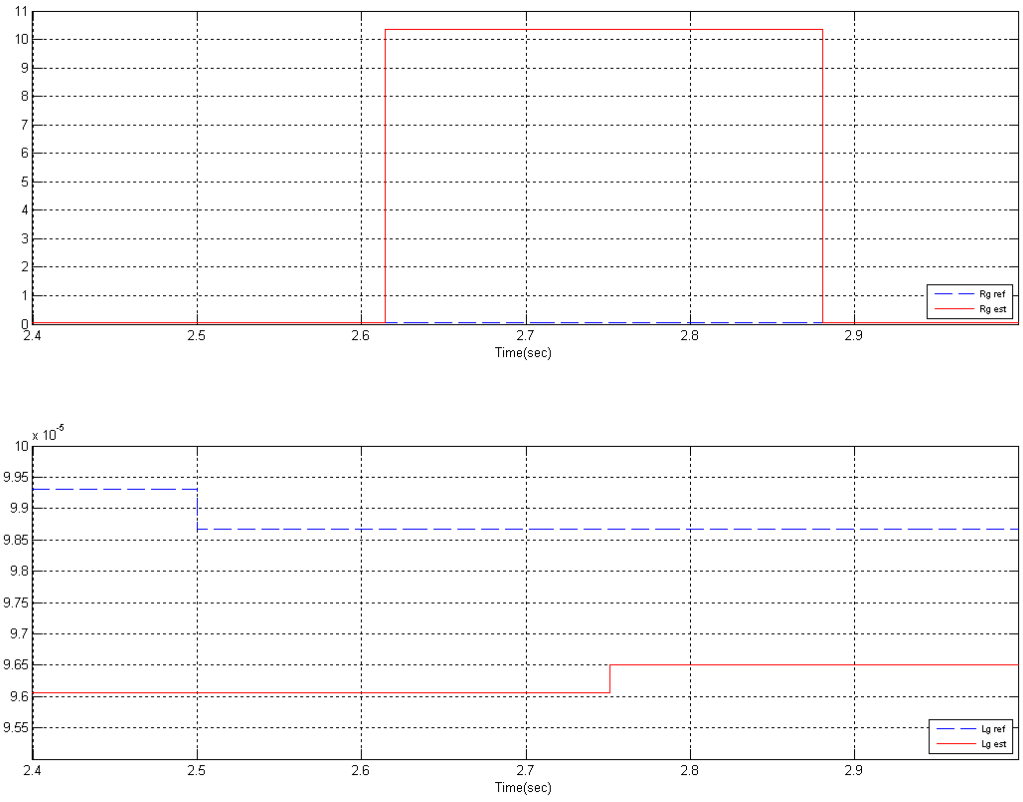

Fig. 4.4: The estimated R_g and L_g signals

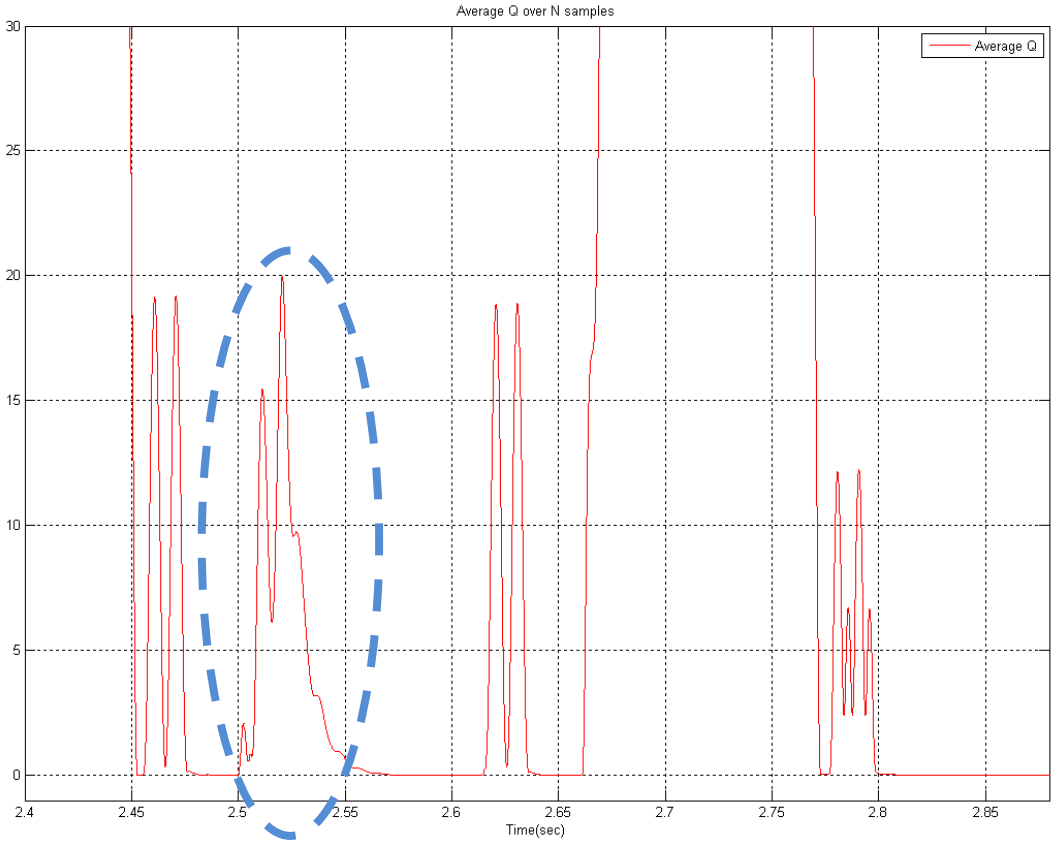

Fig. 4.5: The mean value over N (=500) samples of the reactive power (absolute value). The large transient is highlighted

The modified PQ Variation method simply discards the estimation process if a high transient is detected.

The lower and upper thresholds used in the simulation are 1 and 5 respectively

By analyzing the figure 4.6 is clear how the average reactive power is maintained below a certain level and only at 2.5s a big transient appears; the instantaneous current I_d shows better the effect of the *controlled low slope* ramp active power perturbation. In effect, the controlled ramp is obtained by decreasing (increasing) the active (reactive) power any time the reactive power is less or equal than the lower threshold.

The figure 4.7 shows that it is not necessary to wait the complete impedance estimation process has terminated in order to estimate correctly the line resistance but only a single component estimation interval is needed.

The mean value over N samples of the absolute reactive power value is shown in the figure 4.8.

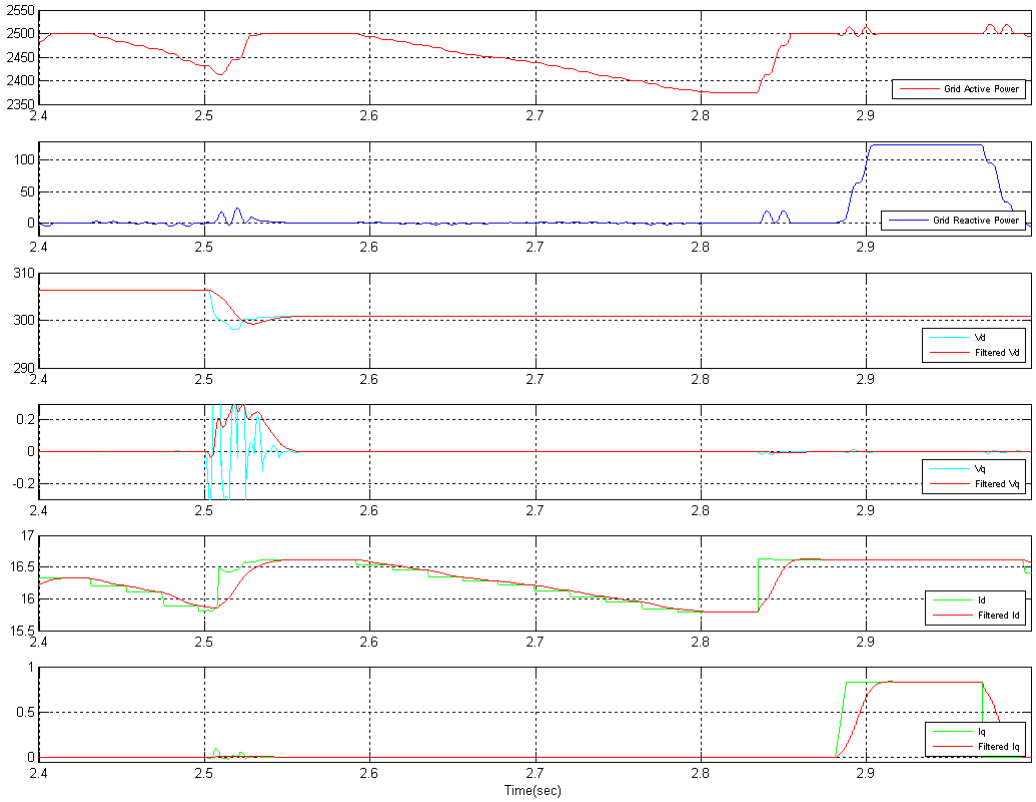

Fig. 4.6 The complete grid impedance estimation process when a micro-grid' features variation happens at 2.5s

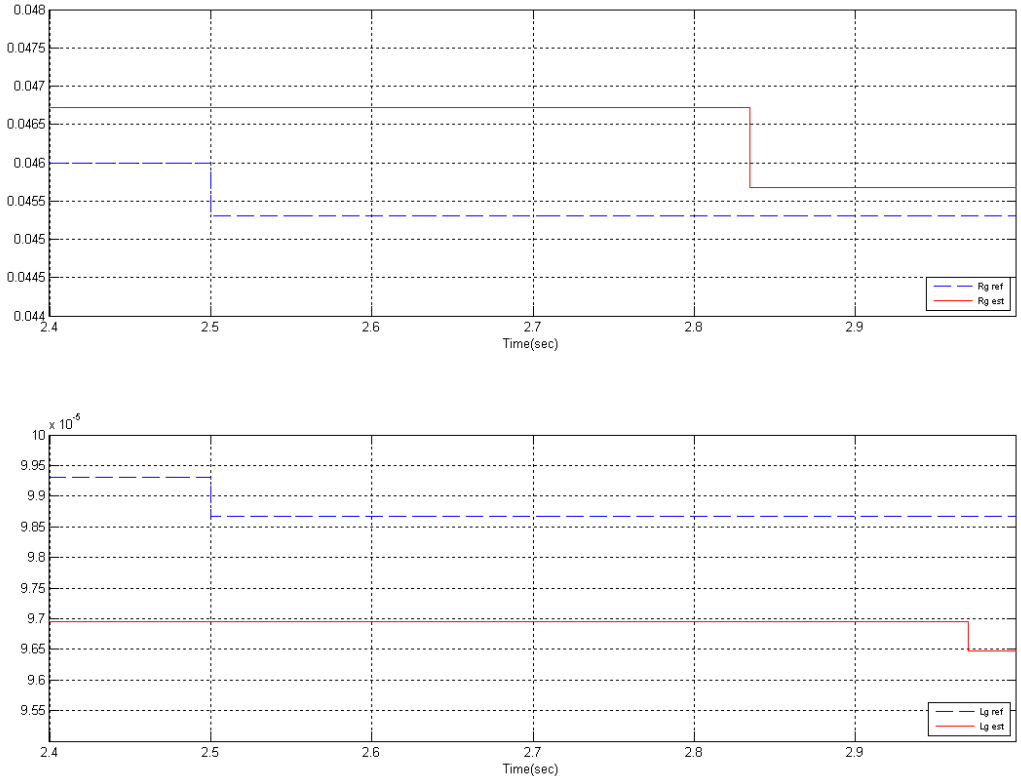

Fig. 4.7 The estimated Rg and Lg: at 2.5s, when a grid change occurs, the resistance estimation process is stopped.

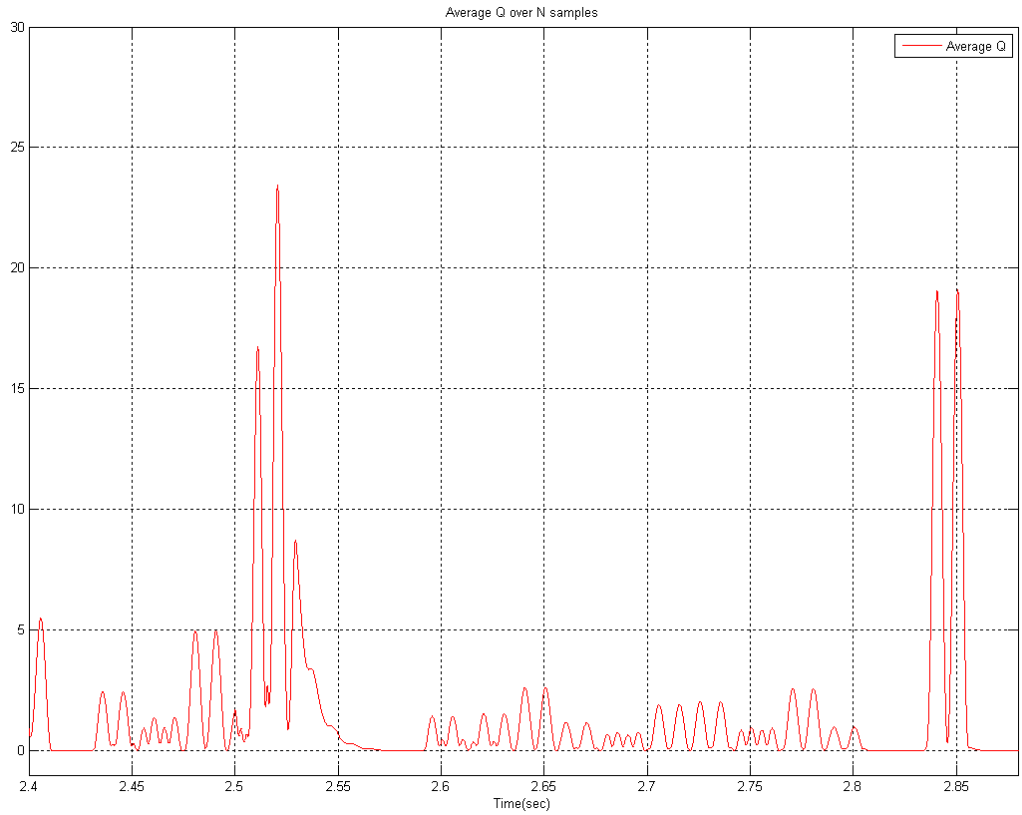

Fig. 4.8: The mean value over N (=500) samples of the reactive power (absolute value). Notice the difference between the reactive transient and the reactive power trend during the power perturbation.

This new proposal is mainly characterized by the following limits:

- The performances of this method are strictly linked to the choice of reactive power thresholds.
- It doesn't take into account possible disturbs due to the inverter or the PV system itself.
- The duration of the estimation process is not fixed and, using the proposed method, it cannot be previously calculated.
- In a switched model, the number N used to average the reactive power could affect the spike detection.

4.3 Final remarks and future works

The PQ Variation Method proposed by Ciobotaru *et al.* in their paper [5] and its possible Simulink-based approach have been illustrated: both the switched and average model has been considered.

The influences of inverter disturbances and of the chosen parameters (such as the DC-link capacitor and the amount of power perturbation) on the method performances have been discussed.

The PQ Variation Method has been checked to have a good accuracy. Indeed, the accuracy of the method is strictly linked to the possible reactive power transients.

The limitations of standard method have been analyzed and, in order to overcome them, a modified PQ Variation method based on the analysis of effects of a micro-grid topology change at the Point of Common Coupling and a possible Simulink-based implementation have been presented. Some limitation of the new proposal has been highlighted: in particular, the effect of bad chosen threshold values could affect both the timing and the accuracy of the modified method.

At present, no algorithm has been defined in order to determine the most appropriate values for both the thresholds.

Following the ideas present in this Thesis, some possible future developments are related to the need to solve many problems that affect the illustrated PQ method for the grid impedance estimation in the single-phase systems.

In particular, as regards the new proposal, an adaptive and fast algorithm to choose the threshold values should be developed and the effects of internal disturbances should be analyzed in order to make the system sensitive only to the external events.

At the end, it could be interesting to apply simultaneously the (standard or modified) PQ variation method at two or more nodes in a micro-grid and to analyze how the method's performances at these nodes are affected by their simultaneous power perturbations.

Appendix

This additional part contains all the programming code of implemented Embedded Matlab® Functions.

Even if some block is very easy to be rebuild, all the functions will be described in order to put in evidence something or to be more easily and easily analyzed.

The following block codes will be examined:

A.1 The *Ialphabeta* block

A.2 The *DQ_voltages* and *DQ_currents* blocks

A.3 The *DeltaxRg* and *DeltaxLg* blocks: remember the only difference between the switched and the average model are the timing parameters.

A.4 The *Rg_ext* and *Lg_ext* blocks

A.5 The *amplitude* measurement block

A.1 The *Ialphabeta* block

The following code is used by this block:

```
function [Ialpha_s,Ibeta_s] = Ialphabeta(Ps,Qs,Valpha_s,Vbeta_s)
%# Reference current generation

Vab=sqrt(Valpha_s^2+Vbeta_s^2);
if(Vab==0 || isnan(Vab))
    Vab=311.1;
end

Ialpha_s=2*(Vbeta_s*Qs+Valpha_s*Ps)/Vab^2;
Ibeta_s=2*(Vbeta_s*Ps-Valpha_s*Qs)/Vab^2;

if(isnan(Ialpha_s) || isnan(Ibeta_s))
Ialpha_s=0;
Ibeta_s=0;
end
```

A.2 The *DQ_voltages* and *DQ_currents* blocks

The following code is used by the *DQ_voltages* block:

```
function [Vd,Vq] = DQ_voltages(cosine,sine,Valpha,Vbeta)
%#

Vd=Valpha*cosine+Vbeta*sine;
```

```
Vq=-Valpha*sine+Vbeta*cosine;

if(isnan(Vd))
    Vd=0.0001;
end

if(isnan(Vq))
    Vq=0.0001;
end

if(isinf(Vd))
    Vd=1e10;
end

if(isinf(Vq))
    Vq=1e10;
end
```

The following code is used by the *DQ_currents* block:

```
function [Id,Iq] = DQ_currents(cosine,sine,Ialpha_s,Ibeta_s)
%#

Id= +Ialpha_s * cosine + Ibeta_s * sine;
Iq= -Ialpha_s * sine + Ibeta_s * cosine;

if(isnan(Id))
    Id=0;
end

if(isnan(Iq))
    Iq=0;
end

if(isinf(Id))
    Id=1e10;
end

if(isinf(Iq))
    Iq=1e10;
end
```

A.3 The *DeltaxRg* and *DeltaxLg* blocks

The following code is used by the *DeltaxRg* block:

```
function [DId,DIq,DVd,DVq] = DeltaxRg(Id,Iq,Vd,Vq,CLK)
%#
persistent Id_ref;
persistent Iq_ref;
persistent Vd_ref;
persistent Vq_ref;

persistent id1;
persistent iq1;
persistent vd1;
persistent vq1;

if(isempty(Id_ref))
    Id_ref=0;
end

if(isempty(Iq_ref))
    Iq_ref=0;
```

```
end

if(isempty(Vd_ref))
    Vd_ref=0;
end

if(isempty(Vq_ref))
    Vq_ref=0;
end


if(isempty(id1))
    id1=0;
end

if(isempty(iq1))
    iq1=0;
end

if(isempty(vd1))
    vd1=0;
end

if(isempty(vq1))
    vq1=0;
end

offset=0.4;

if(CLK < offset)
    Id_ref=Id;
    Iq_ref=Iq;
    Vd_ref=Vd;
    Vq_ref=Vq;
end

if(CLK < 0.1 + offset)
    id1=Id;
    iq1=Iq;
    vd1=Vd;
    vq1=Vq;
end

DId = Id_ref - id1;
DIq = Iq_ref - iq1;
DVd = Vd_ref - vd1;
DVq = Vq_ref - vq1;
```

The following code is used by the *DeltaxLg* block:

```
function [DId,DIq,DVd,DVq] = DeltaxLg(Id,Iq,Vd,Vq,CLK)
%#
persistent Id_ref;
persistent Iq_ref;
persistent Vd_ref;
persistent Vq_ref;

persistent id1;
persistent iq1;
persistent vd1;
persistent vq1;

if(isempty(Id_ref))
    Id_ref=0;
end

if(isempty(Iq_ref))
    Iq_ref=0;
end

if(isempty(Vd_ref))
    Vd_ref=0;
```

```
end

if(isempty(Vq_ref))
    Vq_ref=0;
end


if(isempty(id1))
    id1=0;
end

if(isempty(iq1))
    iq1=0;
end

if(isempty(vd1))
    vd1=0;
end

if(isempty(vq1))
    vq1=0;
end

offset=0.4;

if(CLK < offset )
    Id_ref=Id;
    Iq_ref=Iq;
    Vd_ref=Vd;
    Vq_ref=Vq;
end

if(CLK < offset + 0.1 + 0.15 )
    id1=Id;
    iq1=Iq;
    vd1=Vd;
    vq1=Vq;
end

DId = -Id_ref + id1;
DIq = -Iq_ref + iq1;
DVd = -Vd_ref + vd1;
DVq = -Vq_ref + vq1;
```

A.4 The *Rg_ext* and *Lg_ext* blocks

The following code is used by the *Rg_ext* block:

```
function Rg_ext = Rg_ext(DId,DIq,DVd,DVq)
%#eml

Rg_ext=(DVd*DId+DVq*DIq)/(DId^2+DIq^2);
```

The following code is used by the *Lg_ext* block:

```
function Lg_ext = Lg_ext(DId,DIq,DVd,DVq)
%#eml

Lg_ext=-(DVq*DId-DVd*DIq)/(DId^2+DIq^2)/(100*pi);
```

A.5 The *Amplitude* measurement block

```
function A = Amplitude(x,clk)
%#
persistent m0;
persistent m1;
persistent t0;
persistent t1;

x1=abs(x);

if(isempty(m0))
    m0=0;
end

if(isempty(m1))
    m1=0;
end

if(isempty(t0))
    t0=0;
end

if(isempty(t1))
    t1=0;
end

t0=clk;
if(t0-t1<0.01)
    if(x1>m0)
        m0=x1;
    end
    A=m1;
else
    m1=m0;
    A = m1;
    t1=clk;
    m0=0;
end
```

Bibliography

[1] Jing Yang, Tongwen Chen, Min Wu. *Online Impedance Matrix Estimation of Interconnected Power Systems.* 2009

[2] Marco Liserre, Frede Blaabjerg, Remus Teodorescu. *Grid impedance detection via excitation of LCL-filter resonance.* 2005

[3] Guoqiao Shen, Jun Zhang, Xiao Li, Chengrui Du, Dehong Xu. *Current control optimization for grid-tied inverters with grid impedance estimation.* 2010

[4] Roberto Petrella, Alessandro Revelant, Piero Stocco. *Advances on inter-harmonic variable-frequency injection-based grid-impedance estimation methods suitable for PV inverters.* 2009

[5] Mihai Ciobotaru, Remus Teodorescu, Pedro Rodriguez, Adrian Timbus, Frede Blaabjerg. *Online grid impedance estimation for single-phase grid-connected systems using PQ variations.* 2007

[6] Marco Liserre, Alberto Pigazo, Antonio Dell'Aquila, Victor M. Moreno. *An anti-islanding method for single-phase inverters based on a grid voltage sensorless control.* 2006

[7] Adrian V. Timbusm Pedro Rodriguez, Remus Teodorescu, Mihai Ciobotaru. *Line Impedance Estimation using Active and Reactive Power Variations.* 2007

[8] H. Akagi, Y. Kanazawa, and A. Nabae. *Generalized theory of the instantaneous reactive power in three-phase circuits*, Proc. Int. Power Electron. Conf. (JIEE IPEC), pp.1375 - 1386, 1983.

[9] H. Akagi, S. Ogasawara. *The theory of instantaneous power in three-phase four-wire systems: a comprehensive approach.* 1999

[10] Jacques L. Willems. *A new interpretation of the Akagi-Nabae power components for non-sinusoidal three-phase situations.* 1992